Unexpected Synthesis of Segmented Poly(hydroxyurea–urethane)s from Dicyclic Carbonates and Diamines by Organocatalysis

Amaury Bossion, Roberto H Aguirresarobe, Lourdes Irusta, Daniel Taton, Henri Cramail, Etienne Grau, David Mecerreyes, Cui Su, Guoming Liu, Alejandro J. Müller, et al.

Unexpected Synthesis of Segmented Poly(hydroxyurea–urethane)s from Dicyclic Carbonates and Diamines by Organocatalysis

Amaury Bossion, Roberto H. Aguirresarobe, Lourdes Irusta, Daniel Taton, Henri Cramail, Etienne Grau, David Mecerreyes, Cui Su, Guoming Liu, Alejandro J. Müller, Haritz Sardon*

Abstract

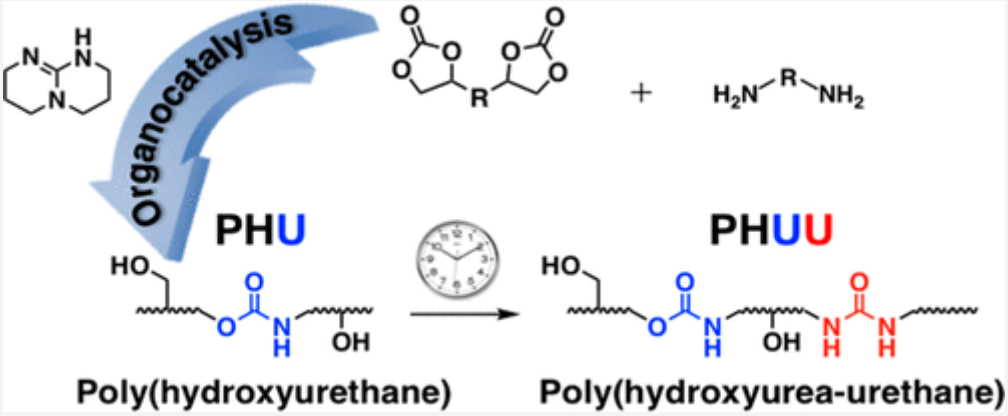

A complete study of the effect of different organocatalysts on the step-growth polyaddition of a five-membered dicyclic carbonate, namely diglycerol dicarbonate, with a poly(ethylene glycol)-based diamine in bulk at 120 °C was first carried out. The reaction was found to be dramatically catalyst-dependent, higher rates being observed in the presence of strong bases, such as phosphazenes (*t*-Bu-P_4 or P_4) and 5,7-triazabicyclo[4.4.0]dec-5-ene (TBD). Unexpectedly, the as-formed urethane linkages entirely vanished with time, as evidenced by FTIR and ^{13}C NMR spectroscopies, while signals due to urea bond formation progressively appeared. An advantage of the chemical transformation occurring from urethane to urea linkages was further taken by optimizing the polymerization conditions to access a range of poly(hydroxyurea–urethane)s (PHUUs) with precise urethane to urea ratio in a one-pot process. Characterization of the corresponding polymers by rheological measurements showed that the storage modulus reached a plateau at high temperatures and at high urea contents. The application temperature range of poly(hydroxyurea–urethane)s could thus be increased from 30 to 140 °C, as for regular polyurethanes. Furthermore, SAXS and phase-contrast microscopy images demonstrated that increasing the urea content improved the phase separation between soft and hard segments of these PHUUs. Altogether, this novel, straightforward, efficient, and environmentally friendly strategy enables the access to non-isocyanate poly(urea–urethane)s with tunable urethane-to-urea ratio from five-membered dicyclic carbonates following an organocatalytic pathway.

1. Introduction

Non-isocyanate polyurethanes (NIPUs) have emerged as a greener alternative to conventional polyurethanes.(1−5) Different synthetic strategies to NIPUs have been developed, including the step-growth polycondensation between activated dicarbonates and diamines or, similarly, between activated dicarbamates and diols.(6,7) Most of the current works dedicated to isocyanate-free polyurethane synthesis are based on the step-growth polyaddition of bifunctional cyclic carbonates with diamines, which results in polyhydroxyurethanes (PHUs). In this context, five- and six-membered dicyclic carbonate monomers have been the most studied.(8−20) While six-membered carbonates prove more reactive than five-membered ones, their

synthesis generally requires the use of chlorinated carbonylating agents, such as phosgene or alkyl chloroformates.(21−23) On the other hand, five-membered cyclic carbonates can be produced in a sustainable way from the chemical insertion of CO_2 into naturally abundant epoxides.(24−31) Although some authors have recently reported the synthesis of high molecular weight NIPUs at room temperature using activated five-membered cyclic carbonate with limited side-reactions, NIPU synthesis from five-membered cyclic carbonates often requires high reaction temperatures, bulk conditions, long reaction times, and, last but not least, the use of a catalyst to achieve high molecular weights.(32,33) Andrioletti and co-workers recently reported a rational study about the aminolysis of five-membered monocyclic carbonates using different organocatalysts. Their screening revealed that 1,5,7-triazabicyclo[4.4.0]dec-5-ene (TBD) and the cyclohexylphenylthiourea could efficiently catalyze the reaction of poorly reactive amines at room temperature.(34) Nevertheless, detailed investigations into the effect of the (organo)catalysts on the final properties of the resulting PHUs remained very scarce. Henderson and co-workers confirmed that TBD enabled to catalyze PHU synthesis from five-membered cyclic carbonates.(10) This prompted us to rationalize the effect of both a structural variation of organocatalysts and experimental conditions on the reaction outcomes and to probe the underlying reaction mechanisms.

Poly(urea–urethane)s (PUUs) are important polymeric materials generally exhibiting high toughness and extensibility; they are extensively used in the textile industry (Lycra DuPont de Nemours and Co.), in foams, and for medical prostheses.(35,36) PUUs combine the processability of polyurethanes with the superior mechanical and thermal properties of polyureas that are imparted primarily by the stronger hydrogen bonding ability of urea moieties relatively to urethanes.(37) Whereas PUUs can be readily synthesized from isocyanate precursors with polyamines, there is only one report dealing with the synthesis of a PUU following a non-isocyanate route, namely, by melt transurethane polycondensation reaction.(38) In addition, the few works having reported the preparation of isocyanate-free ureas have not employed cyclic carbonates.(39,40)

In this work, we propose a novel synthetic approach to non-isocyanate poly(hydroxyurea–urethane)s (PHUUs) that are characterized by a tunable urethane-to-urea ratio. For this purpose, industrially scalable five-membered dicyclic carbonates have been used as key monomer building blocks with a diamine in the presence of various organocatalysts, i.e., following a metal-free route. We have indeed discovered that PHUUs can be effectively achieved via a two-step process, involving the prior formation of hydroxyurethane linkages and their partial postchemical modification into urea moieties. The final urethane-to-urea ratio strongly depends on the organocatalyst and the overall reaction conditions. These observations are supported by results obtained from model reactions with monofunctional substrates, which allows us to propose a reaction mechanism pertaining to this unexpected chemical transformation in the presence of peculiar organocatalysts. To the best of our knowledge, this is the first report on PHUU synthesis via an organocatalyzed step-growth polyaddition of diamines with five-membered dicyclic carbonates.

2. Experimental Section

2.1. Instrumentation and Materials

Nuclear Magnetic Resonance (NMR)

^{1}H and ^{13}C spectra were recorded with Bruker Avance DPX 300 or Bruker Avance 400 spectrometers. The NMR chemical shifts were reported as δ in parts per million (ppm) relative to the traces of nondeuterated solvent (e.g., δ = 2.50 ppm for d_6-DMSO or δ = 7.26 for $CDCl_3$). Data were reported as chemical shift, multiplicity (s = singlet, d = doublet, t = triplet, m = multiplet, br = broad), coupling constants (*J*) given in hertz (Hz), and integration.

Size Exclusion Chromatography (SEC)

SEC was performed in THF at 30 °C using a Waters chromatograph equipped with four 5 mm Waters columns (300 mm × 7.7 mm) connected in series with increasing pore sizes (100, 1000, 105, and 106 Å). Toluene was used as a marker. Polystyrenes of different molecular weights, ranging from 2100 to 1 920 000 g mol^{-1}, were used for the calibration.

Fourier Transform Infrared (FT-IR) Spectroscopy

FT-IR spectra were obtained by FT-IR spectrophotometer (Nicolet 6700 FT-IR, Thermo Scientific Inc., USA) using the attenuated total reflectance (ATR) technique (Golden Gate, spectra Tech). Spectra were recorded between 4000 and 525 cm^{-1} with a spectrum resolution of 4 cm^{-1}. All spectra were averaged over 10 scans.

Differential Scanning Calorimetry

A differential scanning calorimeter (DSC-Q2000, TA Instruments Inc., USA) was used to analyze the thermal behavior of the samples. A total of 6–8 mg of samples was first scanned from −80 to 150 °C at a heating rate of 20 °C min^{-1} to eliminate interferences due to moisture. The samples were then cooled to −80 °C to remove the thermal history and reheated to 150 °C at 20 °C min^{-1}. The glass transition and melting temperatures were calculated from the second heating run.

Elemental Analysis

The elemental analysis for carbon, hydrogen, and nitrogen content was performed using a Leco TruSpec Micro instrument (Germany) at 1000 °C using helium as transport gas. The analysis was conducted twice for comparison using 1–2 mg of sample.

Mass Spectroscopy (LC-TOF-MS)

The mass spectroscopy analysis consisted of a chromatographic separation in an ultrahigh performance liquid chromatograph (UPLC, Acquity system from Waters Cromatografia S.A., USA) coupled to a high-resolution mass spectrometer (Synapt G2 from Waters Cromatografia S.A., USA, time-of-flight analyzer (TOF)) by an electrospray ionization source in positive mode (ESI). The chromatographic separation was achieved using an Acquity UPLC BEH C18 column (1.7 µm, 2.1 × 50 mm i.d.) with an Acquity UPLC BEH C18 1.7 µm VanGuard precolumn (2.1 × 5 mm) (Waters Cromatografia S.A., USA) and a binary A/B gradient (solvent A: water with 0.1% formic acid; solvent B: methanol with 0.1% formic acid). The gradient program was established as follows: initial conditions were 5% B, raised to 100% B over 2.5 min, held at 100% B until 4 min, decreased to 5% B over the next 0.1 min, and held at 5% B until 5 min for re-equilibration of the system prior to the next injection. A flow rate of 0.25 mL/min was used, the column temperature was 30 °C, the autosampler temperature was 4 °C , and the injection volume was 7.5 µL. High-resolution mass data were acquired in SCAN mode, using a mass range 50–1200 u in resolution mode (fwhm ≈ 20 000) and a scan time of 0.1 s. The source temperature was set to 120 °C and the desolvation temperature to 300 °C. The capillary voltage was 0.5 kV and the cone voltage 15 V. Nitrogen was used as the desolvation and cone gas at flow rates of 800 and 10 L/h, respectively. Before analysis, the mass spectrometer was calibrated with a sodium formate solution. A leucine–enkephalin solution was used for the lock mass correction, monitoring the ions at mass-to-charge ratio (*m*/*z*) 556.2771 and 278.1141. All of the acquired spectra were automatically corrected during acquisition based on the lock mass. The sample was dissolved in acetone at 65 °C and diluted in methanol for the analysis (around 20 µg/mL).

Rheometry Measurements

Small-amplitude oscillatory experiments were performed in a stress-controlled Anton Paar Physica MCR101 rheometer, and the experiments were carried out using 25 mm parallel plate geometry. All the experiments

were conducted in linear viscoelastic conditions for the studied temperature range (strain = 0.5% and frequency 1 Hz).

Small-Angle X-ray Scattering (SAXS)

SAXS experiments were carried out on a Xeuss SAXS/WAXS system (Xenocs SA, France). A multilayer focused Cu Kα X-ray source (GeniX3D Cu ULD), generated at 50 kV and 0.6 mA, was employed. The wavelength of the X-ray radiation was 0.154 18 nm. A semiconductor detector (Pilatus 300K, DECTRIS, Swiss) with a resolution of 487 × 619 pixels (pixel size 172 × 172 μm^2) was applied to collect the scattering signals. The exposure time for each SAXS pattern was 30 min. The one-dimensional scattering intensity profiles were integrated after background correction from 2D SAXS patterns.

Optical Microscopy

The phase morphology of the samples was observed with a phase contrast microscope (Olympus BX51, Japan) equipped with a Linkam THMS600 hotstage (Linkam Scientific Instruments, UK).

Reagents

1,5,7-Triazabicyclo[4.4.0]dec-5-ene (98%) (TBD), 1,12-diaminododecane (98%), *N*-butylamine (99.5%), *O*,*O*'-bis(2-aminopropyl)polypropylene glycol-*block*-poly(ethylene glycol)-*block*-polypropylene glycol (Jeffamine ED-2003) with a molecular weight around 1900 g mol^{-1}, *p*-toluenesulfonic acid monohydrate (98.5%) (PTSA), phosphazene base P_4-*t*-Bu solution (0.8 M solution in hexane) (P_4), and sodium methoxide (95%) were purchased from Sigma-Aldrich. 1,8-Diazabicyclo[5.4.0]undec-7-ene (≥98%) (DBU) and diglycerol (≥80%) were purchased from TCI Chemicals. 3,5-Bis(trifluoromethyl)phenyl isothiocyanate (99%), hexane (laboratory reagent grade), methanol (analytical reagent grade), and tetrahydrofuran (analytical reagent grade) were purchased from Fisher. Dimethyl carbonate (extra dry, ≥99%), dodecylamine (98%), and propylene carbonate (99.5%) were purchased from Acros Organics. Deuterated solvents such as $CDCl_3$ and d_6-DMSO was purchased from Euro-top. All materials were used without further purification.

2.2. Synthesis of Diglycerol Dicarbonate (DGC)

Synthesis of DGC was carried out in an adapted version of Van Velthoven et al.(41) In a 500 mL round-bottom flask equipped with a magnetic stirrer and a condenser, diglycerol (1 equiv, 23.18 g, 0.14 mol) and sodium methoxide (0.05 equiv, 0.38 g, 7 mmol) were added to a solution of dimethyl carbonate (10 equiv, 125.6 g, 117.5 mL, 1.4 mol) under a nitrogen atmosphere. The reaction mixture was heated under reflux for 48 h. After cooling down to room temperature, the reaction was filtrated and concentrated under vacuum. After evaporation of dimethyl carbonate, the product was crystallized in methanol at −80 °C. DGC was obtained as a white powder after drying in the vacuum oven at 40 °C for 24 h (11.79 g, 39% yield). The structure was confirmed by ^{1}H and ^{13}C NMR spectroscopy. ^{1}H NMR (300 MHz, d_6-DMSO, δ): 4.97–4.91 (m, 1H), 4.52 (t, J = 8.5 Hz, 1H), 4.27–4.21 (m, 1H), 3.78–3.75 (m, 1H), 3.74–3.66 (m, 1H). ^{13}C NMR (75 MHz, d_6-DMSO, δ): 154.84, 75.40, 75.34, 70.39, 70.35, 65.88. IR (ATR, cm^{-1}): 2998, 2927, 2888, 1765, 1546, 1481, 1371, 1340, 1259, 1168, 1112, 1058, 956, 845, 801, 769, 711. Characterization data are consistent with previous reports.(41−43)

2.3. Synthesis 1-(3,5-Bis(trifluoromethyl)phenyl)-3-butylthiourea (TU)

Synthesis of TU was carried out following the procedure described elsewhere.(44) Butylamine (1.61 g, 22.1 mmol) was added dropwise at room temperature to a stirred solution of 3,5-bis(trifluoromethyl)phenyl isothiocyanate (5 g, 18.44 mmol) in dry THF (50 mL). The solution was left stirring for another 4 h at room temperature. The reaction mixture was concentrated under vacuum, and the product was recrystallized from hexane. After drying under vacuum, TU was obtained as a slightly yellow powder (5.89 g, 92% yield). The structure was confirmed by ^{1}H NMR spectroscopy. ^{1}H NMR (300 MHz, d_6-DMSO, δ): 9.88 (s, 1H), 8.23 (s, 2H),

7.72 (s, 1H), 3.49 (t, 2H), 1.55 (m, 2H), 1.33 (m, 2H), 0.91 (t, *J* = 7.3 Hz, 3H). Characterization data are consistent with a previous report.(44)

2.4. General Procedure for Polymerization Reactions

In a typical procedure, DGC (1 equiv), diamine (1 equiv), and catalyst (0.1 equiv) were mixed together in a 25 mL vial equipped with a magnetic stirrer. The polymerization reaction was conducted at 120 °C under stirring and under ambient atmosphere. Aliquots were taken at regular intervals for FTIR-ATR, NMR, DSC, and SEC analyses.

2.5. General Procedure for Model Reaction

In a typical procedure, propylene carbonate (1 equiv, 7 mmol), dodecylamine (1 equiv, 7 mmol), and catalyst (0.1 equiv, 0.7 mmol) were mixed together in a 25 mL vial equipped with a magnetic stirrer. The reaction was conducted at 120 °C under stirring and ambient atmosphere for 24 h. Aliquots were taken at specific intervals of time for FTIR-ATR, NMR, elemental analysis, and LC-TOF-MS.

2.6. General Procedure for Urea Formation from Hydroxyurethane

In this procedure, propylene carbonate (1 equiv, 7 mmol) and dodecylamine (1 equiv, 7 mmol) were mixed together in a 25 mL vial equipped with a magnetic stirrer. The reaction was conducted at 120 °C for 53 h in two parts. First, the reaction was let under stirring at 120 °C until complete conversion of propylene carbonate. Then, TBD (0.1 equiv, 0.7 mmol) was added in the medium, and the reaction was left stirring at 120 °C for 48 h. Aliquots were taken after 5 h (without TBD) and 48 h (with TBD) for FTIR and ^{1}H NMR spectroscopy analyses.

3. Results and Discussion

3.1. Effect of Organocatalysts on the Polymerization Kinetics during Polyhydroxyurethane Synthesis

Different organocatalysts were screened for the step-growth polyaddition of diglycerol dicarbonate (DGC) and Jeffamine ED-2003 (M_n = 1900 g mol^{-1}) (Scheme 1a). On one hand, DGC was selected because it can be easily prepared from bio-based diglycerol and dimethyl carbonate with no side-reactions. On the other hand, a low molecular weight propylene oxide capped poly(ethylene glycol)-based diamine (Jeffamine ED-2003) was selected as diamine since it enables the formation of soft polyhydroxyurethanes that can be further analyzed by ^{1}H NMR. In addition, Jeffamine is analogous to poly(ethylene glycol)s (PEGs) commonly employed for the polymerization of segmented isocyanate-based polyurethanes.

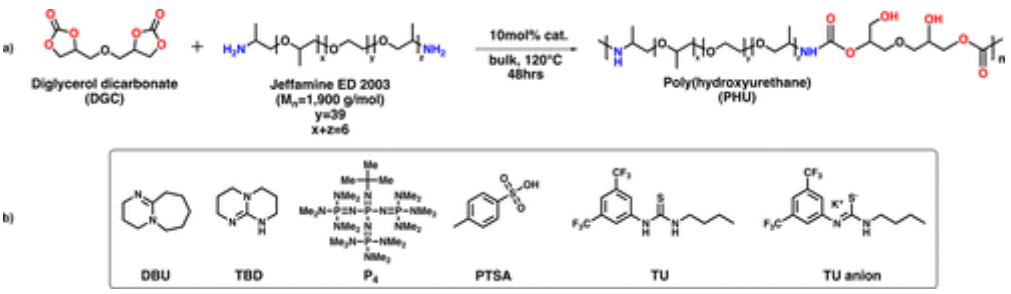

Scheme 1. (a) Step-Growth Polyaddition of DGC with Jeffamine ED-2003; (b) Catalysts Used in This Study

The organocatalysts tested included an organic acid, namely, *p*-toluenesulfonic acid (PTSA), organic bases of different pK_a values, such as diazabicyclo[5.4.0]undec-7-ene (DBU), phosphazene base 1-*tert*-butyl-4,4,4-tris(dimethylamino)-2,2-bis[tris(dimethylamino)phosphoranylidenamino]-2λ^5,4λ^5-catenadi(phosphazene) (P_4), 1,5,7-triazabicyclo[4.4.0]dec-5-ene (TBD), and H-bonding donors such as 1-(3,5-bis(trifluoromethyl)phenyl)-3-butylthiourea (TU) and potassium thioimidate (TU anion) (Scheme 1b). The TU anion was generated by deprotonation in THF of neutral TU with potassium methoxide, as described by Waymouth et al.(45,46) It has

been established that these catalysts operate through specific mechanisms that can enhance the polymerization rate and/or selectivity.(44,45,47−49)

Polymerization studies were performed in bulk at 120 °C by mixing equimolar amounts of DGC and Jeffamine ED-2003, followed by addition of 10 mol % of the catalyst. Monomer conversion was monitored by FTIR-ATR, through the decrease of the relative integration value of the carbonate carbonyl characteristic band at 1780 cm^{-1}. In order to take into account the path length of the samples, the obtained values were normalized to the absorbance of a band whose intensity did not change during the reaction. The total C–H stretching in the range 3000–2850 cm^{-1} was thus selected. Results of these kinetics are shown in Figure 1. The polymerization rate was found to be highly catalyst dependent. In the absence of any catalyst, monomer conversion reached barely 70% after 48 h, and full conversion could not be achieved. The TU anion appeared to be the most efficient catalyst, as monomer conversion reached >98% within 5 min, while only 83 and 45% monomer conversions were observed with P_4 and TBD, respectively. While differences in the reaction rates were observed at the beginning of the polymerization, the three organocatalysts all gave a conversion exceeding 98% within 10 h. DBU and TU, however, did not provide any significant effect, as the reaction did not reach completion even after 48 h (86 and 90% conversion, respectively).

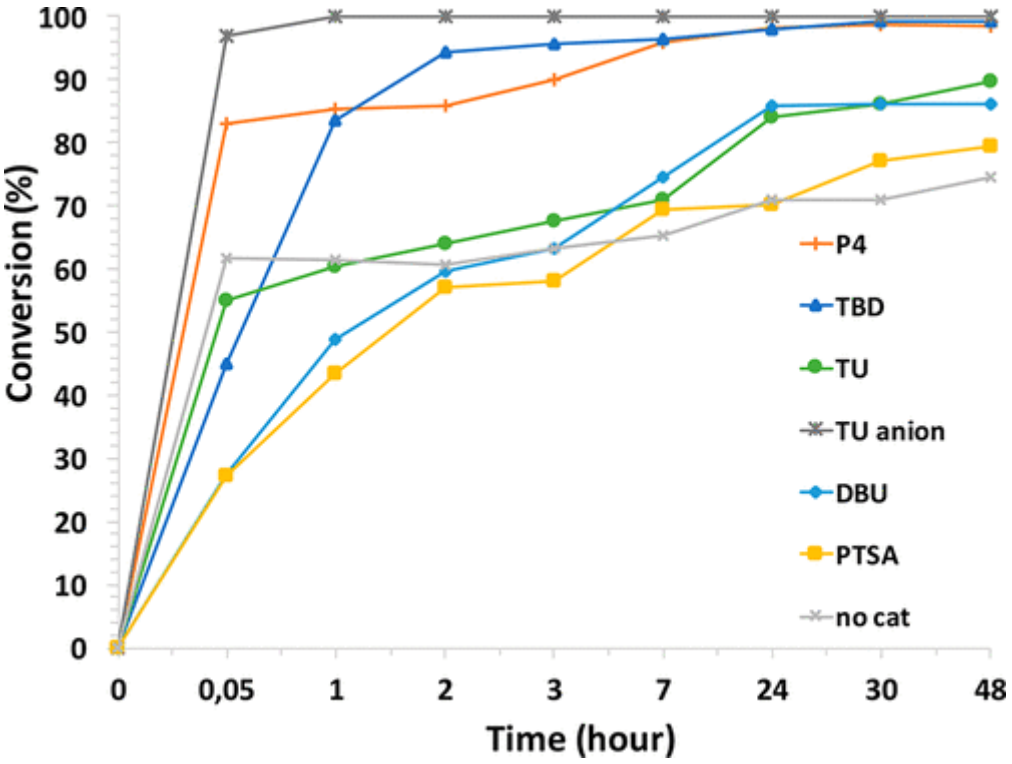

Figure 1. Kinetic plot of the step-growth polymerization of DGC with Jeffamine ED-2003 at 120 °C using different organocatalysts.

As for PTSA, it did not enable to reach a higher conversion than that obtained for the noncatalyzed reaction after 48 h.

Analysis of the carbonyl region of FTIR spectra run at different reaction times for polymers obtained in the presence of the most active catalysts, i.e. P_4, TBD and TU anion (Figure 2 and Figure S20), revealed an intriguing phenomenon. The signal at 1795 cm^{-1} due to the carbonyl group of the starting DGC decreased after 1 h, as expected, while signals attributed to the newly formed urethane bond could be observed at 1715 cm^{-1} (C═O stretching vibration) and 1530 cm^{-1} (N–H bending vibration). Surprisingly, a new signal appeared at 1670 cm^{-1} as the reaction proceeded (10 h) that was attributed to the C═O stretching vibration of urea groups. After 48 h of reaction, the urethane band continued to decrease in intensity, and the signal of the urea groups became

predominant in the carbonyl region. In addition, the latter signal evolved to lower wavenumbers (1650 cm^{-1}), and the N–H deformation vibration was recorded at higher wavenumbers (1550 cm^{-1}). With DBU, PTSA, and TU as well as without catalyst, this behavior was not observed at this temperature.

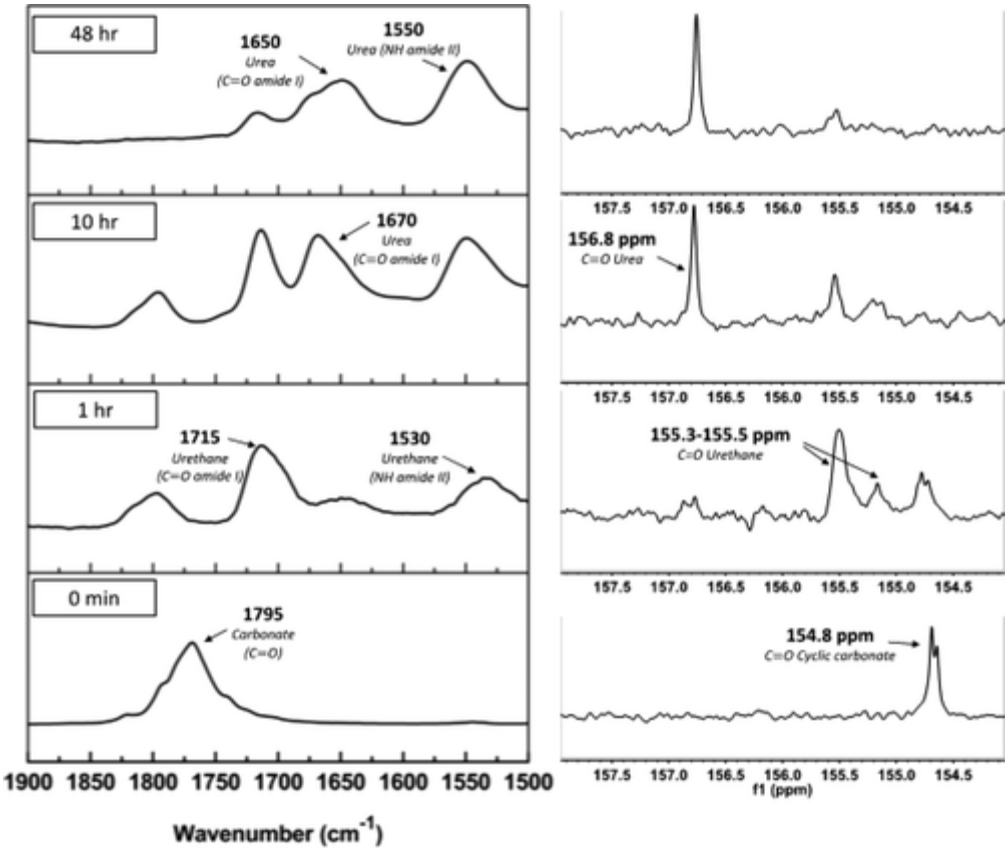

Figure 2. FTIR (left) and ^{13}C NMR (d_6-DMSO, right) spectra of products obtained at different times from the step-growth polymerization of DGC with Jeffamine ED-2003 performed at 120 °C using TBD as catalyst.

To further confirm the progressive transformation of the polyhydroxyurethane precursors to poly(hydroxyurea–urethane)s (PHUUs), quantitative ^{13}C NMR analysis was performed in the carbonyl region for higher resolution (Figure 2). Polymers were analyzed at different reaction times (1, 10, and 48 h). After 1 h, three different signals can be observed at 154.8, 155.3, and 155.5 ppm, respectively. While the first one is assigned to the DGC C═O group, the second one corresponds to the newly formed (−NH–(C═O)–O−) urethane linkages (containing primary and secondary hydroxyls).(41,42) After 10 h, the area of the signal attributed to the cyclic carbonate decreased, and the new signal appearing at 156.8 ppm can be attributed to the urea (−NH–(C═O)–NH−) carbonyl group. The reaction was confirmed by the complete disappearance of the carbonyl band associated with the five-membered cyclic carbonate monomer. Moreover, the formation of urea bond was also evidenced by ^{1}H NMR, with the disappearance of the urethane NH signal over time at 6.94 ppm and the formation of a new peak at 5.67 ppm corresponding to the urea labile NH proton (Figure S1). In order to speed up the urea formation, polymerization was performed at higher temperature (i.e., 150 °C) using TBD as organocatalyst. Overall, we found that urea formation proceeded faster at 150 °C than at 120 °C (Figure S40). For example, 77% urea was achieved in 2 h at 150 °C while 24 h was required to attain a similar urea ratio at 120 °C.

3.2. Model Reaction

In light of the previous results, a model reaction utilizing propylene carbonate and dodecylamine as monofunctional reaction partners was performed in the presence of TBD as organocatalyst (Figure 3). As

propylene carbonate reacted with dodecylamine, diagnostic ^{1}H NMR signals due to the methylene protons of the cyclic carbonate at 4.96–4.91, 4.52, and 4.27–4.20 ppm disappeared (Figure S2a). Meanwhile, new signals attributed to the urethane moieties were detected at 4.92–4.84 ppm (C*H*–OCONH compound **1**), 4.76 ppm (C*H*–OH compound **1'**), 3.90–4.12 ppm (CH_2–OCONH compound **1'**), 3.55–3.70 ppm (CH_2–OH compound **1**), and 3.16 ppm (CH_2–NHCOO) (Figure S2b). As the reaction proceeded, a clear evolution of the signals due to urethane groups was noted. These signals decreased in intensity, and a new signal due to methylene protons linked to the urea groups appeared at 3.16 ppm (CH_2–NH). In addition, a new peak was observed at 4.30 ppm assigned to protons of the urea group. To our surprise, signals due to methylene protons of the cyclic carbonate reappeared, as a sign of the partial reversion of the process, thus regenerating hydroxyurethane linkages (Figure S2c). Similar findings have actually been reported by Torkelson et al.(50) These authors have indeed found that PHU-based networks are able to dissociate to cyclic carbonates and amine groups, under specific reprocessing conditions. Moreover, we noted that substantial amounts of a condensate formed at the early stages of the reaction.

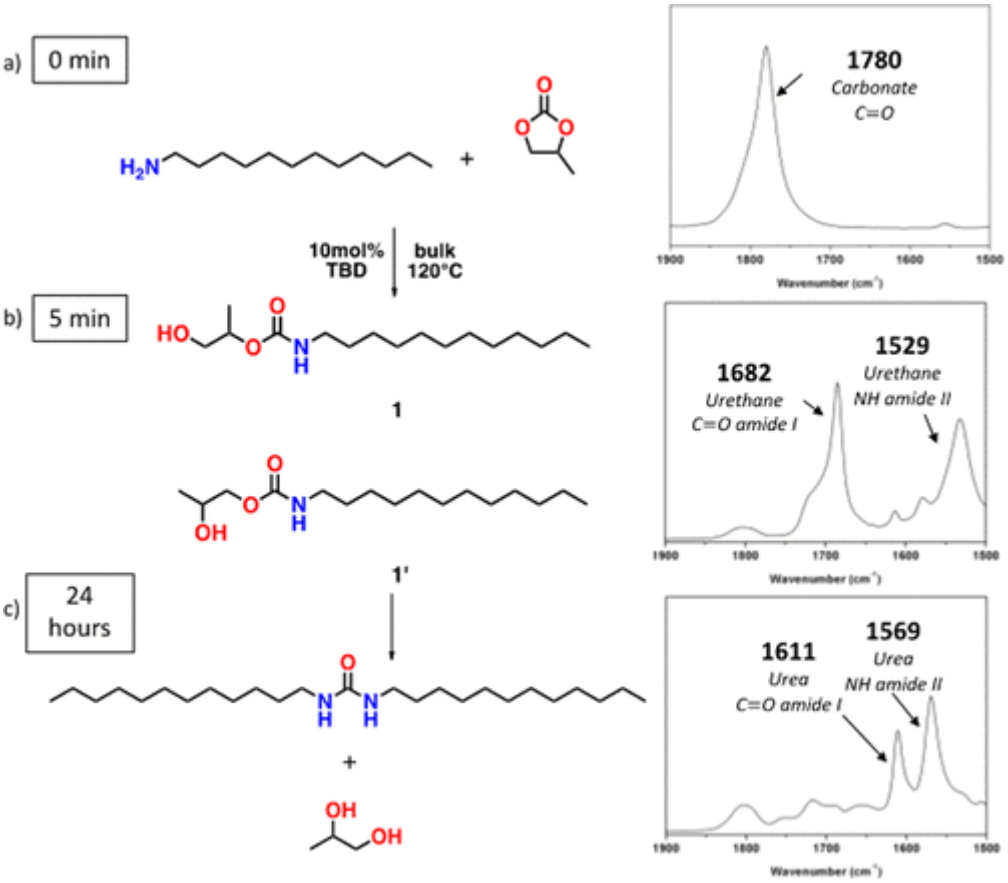

Figure 3. Evolution of the FTIR-ATR spectra with time during the aminolysis of propylene carbonate with dodecylamine at 120 °C using TBD as catalyst.

Analysis by ^{1}H NMR of this condensate revealed that it was propane-1,2-diol as side product, with characteristic peaks at 3.94–3.84 ppm (C*H*–OH), 3.63–3.58 and 3.41–3.35 ppm (CH_2–OH), 2.99 ppm (O*H*), and 1.15 ppm (CH_3) (Figure S3).(51) After 24 h (Figure S2c), peaks due to urethane group completely vanished, and peaks assigned to urea moieties were mainly detected in the ^{1}H NMR.

Urea formation was further analyzed by FTIR-ATR. Similar results to those of the polymerization were observed, i.e., disappearance of urethane moieties and appearance of high intensity signals due to urea groups (Figure 3). In addition, analysis of the FTIR spectra at different reaction times showed that full urea formation was achieved in 24 h, confirming the results obtained by NMR spectroscopy (Figure S23). Elemental and LC-

TOF-MS analyses of the aminolysis of propylene carbonate with dodecylamine after 24 h were conducted to characterize the final compound after its recrystallization in cold chloroform. One main compound was detected at *m*/z = 397.42. The empirical formula proposed for this protonated molecule was $C_{25}H_{53}N_2O$ [M + H^+] matching the structure of 1,3-didodecylurea. In addition, elemental analysis gave experimental values that fitted well with this chemical formula (Figures S34 and S35 and Table S1). These results thus confirmed that organocatalysts such as TBD or P_4 mainly generated urea groups starting from a cyclic carbonate and a primary amine.

Nevertheless, the nearly complete conversion of the cyclic carbonate into urethane followed by urea formation suggested that the reaction mechanism followed a different pathway than the well-established amidation side-reaction of hydroxyurethane with the primary amine.(16)

Recent studies have reported the dissociative reversible aminolysis reaction in PHU reprocessability process; however, no detailed mechanism has been discussed.(50,52) Our study suggests that urea formation occurred in the presence of basic catalysts. A mechanism has been proposed, as illustrated in Scheme 2. It was apparent that urethane groups initially formed from cyclic carbonate and primary amine and further evolved into urea moieties. In the presence of TBD, the hydroxyl group created upon aminolysis might be deprotonated. The newly formed alkoxide might react with the carbonyl electrophilic center of the urethane group. We hypothesize that the mechanism further involves a proton transfer from the catalyst to the urethane amine concomitantly, followed by cleavage of the bond between the amine and the carbonyl carbon, leading to the formation of the cyclic carbonate and the free amine. This reaction was supported by ^{1}H NMR data with the appearance of characteristic signals assigned to the cyclic carbonate monomer (Figure S2). In a second step, the newly formed dodecylamine can either further react with the cyclic carbonate to form the urethane compound again or react with another urethane group to form the linear urea and propane-1,2-diol. In the latter case, the strong base could deprotonate the amine, making it more nucleophilic for an attack onto another urethane linkage and/or facilitate the proton transfer from the amine to the propane-1,2-diol side-product after the cleavage of the urethane bond, yielding the urea. The presence of the two compounds was confirmed by ^{1}H NMR. To further ascertain the base-promoted formation of linear ureas from hydroxyurethanes, the hydroxyurethane synthesized from propylene carbonate and dodecylamine was placed at 120 °C with 10 mol % of TBD. As expected, 1,3-didodecylurea and propylene glycol were thus generated, supporting our hypothesis (Figures S4 and S21). Similarly, preformed polyhydroxyurethane underwent urea formation after 48 h in the presence of 10 mol % TBD, which further strengthen the proposed mechanism (Figure S32).

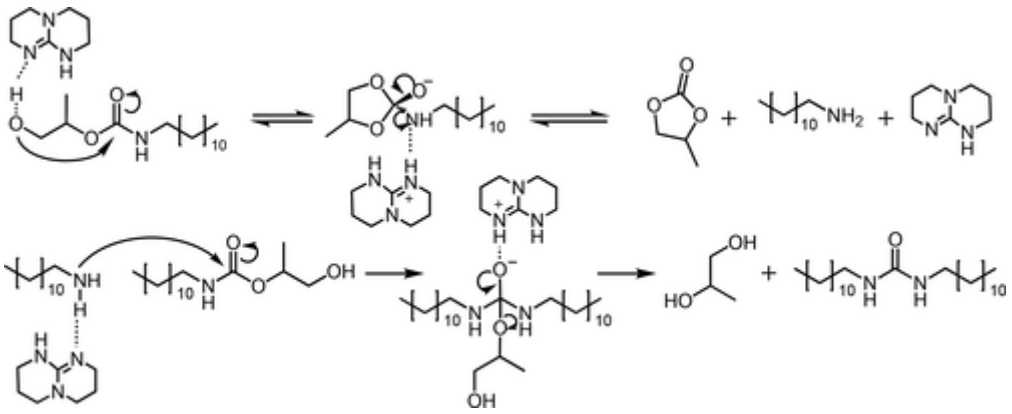

Scheme 2. Proposed Mechanism for the Formation of Urea from Urethane with TBD as Example of Base Catalyst

3.3. Synthesis of Poly(hydroxyurea–urethane)s Based on DGC and Diamines

On the basis of the findings discussed above, the scope of urea formation was expanded to the synthesis of various PHUUs with different urea–urethane ratios, in a one-pot process, from dicyclic carbonates. PUUs are considered as attractive materials owing to the higher resistance of the urea linkage to hydrolysis compared to the urethane one. PUUs also exhibit improved mechanical properties due to the ability of urea groups to form stronger hydrogen bonding compared to polyurethanes.

We thus prepared three different PHUUs with different urethane/urea ratios by polymerizing Jeffamine ED-2003 with DGC at 120 °C in the presence of TBD as catalyst (PHUU1, PHUU2, and PHUU3) by simply discontinuing the reaction at different reaction times (Scheme 2). The urethane/urea ratio was determined by FTIR and ^{1}H NMR (Table1, Figure 4, and Figures S5–S7 and S24–S26).

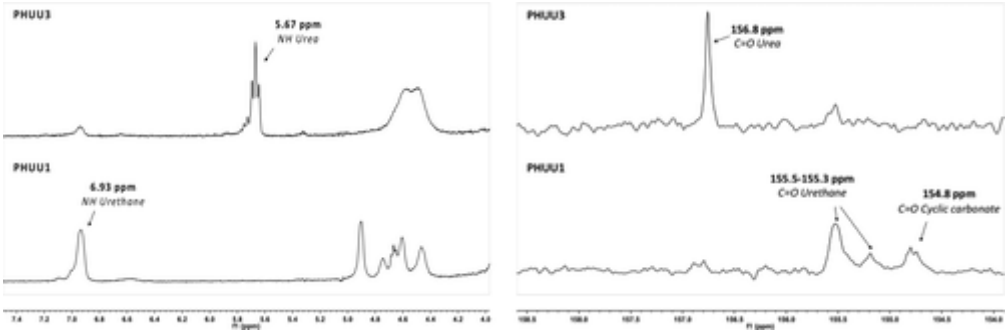

Figure 4. Representative ^{1}H (in the area 4–7.5 ppm, left) and ^{13}C (in the area 154–158.5 ppm, right) NMR of PHUU1 (0% urea) and PHUU3 (83% urea).

Table 1. PHUUs Synthesized from DGC and Diamines at 120 °C Using 10 mol % of TBD as Catalyst

						DSC			SEC		SAXS
PHUU	Jeffamine ED-2003 (mol %)[a]	1,12 diaminododecane (mol %)[a]	PEG content (wt%)	time (hours)	Ratio urethane/urea (%)[b]	T_g (°C)[c]	T_m (°C)[c]	ΔH_m (J.g^{-1})[d]	M_n (g.mol^{-1})[e]	Đ[e]	Long period (nm)
1	100	0	90	1	100/0	-31	33	86	4000	1.8	-
2	100	0	95	10	45/55	-37	32	77	6200	1.6	-
3	100	0	98	48	17/83	-40	32	72	11,200	1.8	-
4	60	40	83	3	100/0	-33	32	93	5700	1.4	11.2
5	60	40	85	10	59/41	-38	30	90	7700	1.7	12.5
6	60	40	87	18	43/57	-39	31	80	8700	1.6	12.5
7	60	40	88	24	32/68	-54	29	76	8400[f]	1.7[f]	10.8
8	60	40	90	48	16/84	-57	28	74	8100[f]	1.6[f]	9.6

[a]Calculated according to the mol % in diglycerol dicarbonate.
[b]Conversions were calculated by FTIR-ATR using the carbonyl characteristic bands of urethane at 1715 cm^{-1} and urea at 1670 cm^{-1}.
[c]Data calculated from the second heating run of the DSC analysis.
[d]Data normalized to the weight fraction of PEG.
[e]M_n values were obtained by SEC in THF; the reported numbers are in reference to polystyrene standards.
[f]The polymers were partially soluble in THF. Analyses were performed after purification of the polymers, performed by dissolving and precipitating in methanol and cold ether, respectively.

The thermal properties of the PHUUs compounds were then analyzed, after purification, by differential scanning calorimetry (Table1 and Figure S38). Low T_g values were observed for PHUU1, PHUU2, and PHUU3 (−31, −37, and −40 °C, respectively), which was related to the presence of the soft Jeffamine segment. Moreover, as the urea content increased, the T_g of the final polymers decreased, which in our opinion may be related to a more pronounced phase separation due to (1) the presence of urea bonds which could form stronger hydrogen bond interaction than urethane groups and (2) because while urea groups were formed hydroxyl pending groups were diminished, reducing the ability of the hard segment to interact with the polyether based soft segment via hydrogen bonding.

Despite their intriguing properties, one limitation of PHUs based on polyether soft segments, with respect to conventional polyurethanes, is their poor mechanical properties at high temperature. This is due to the lower ability to phase separate as strong hydrogen bonding interaction develop between pending hydroxyl groups

and the polyether-based soft segments.(53) As Torkelson et al. have reported, PHUs consisting of oxygen-free soft segments, i.e., made of polybutadiene-*co*-acrylonitrile, exhibit sharper domain interphases, which is explained by a lack of hydrogen bonding between hard and soft segments.(54) Likewise, we expected phase separation to occur with our PHUUs due to the lesser probability for forming hydrogen bonding. The effect of the urea content on the thermomechanical properties was thus investigated with samples prepared from a mixture of two primary amines, namely, the same Jeffamine ED-2003 and 1,12-diaminododecane with a molar ratio = 60/40 (Table1). Five PHUUs were thus synthesized at 120 °C in the presence of 10 mol % of TBD as catalyst, with different urea/urethane ratios (PHUU4, PHUU5, PHUU6, PHUU7, and PHUU8) (Scheme 3). The urethane content was varied from 100% to 16% as determined by FTIR, ^{1}H NMR, and ^{13}C NMR (Figures S27–S31, Figures S8–S13, and Figures S14–S19, respectively).

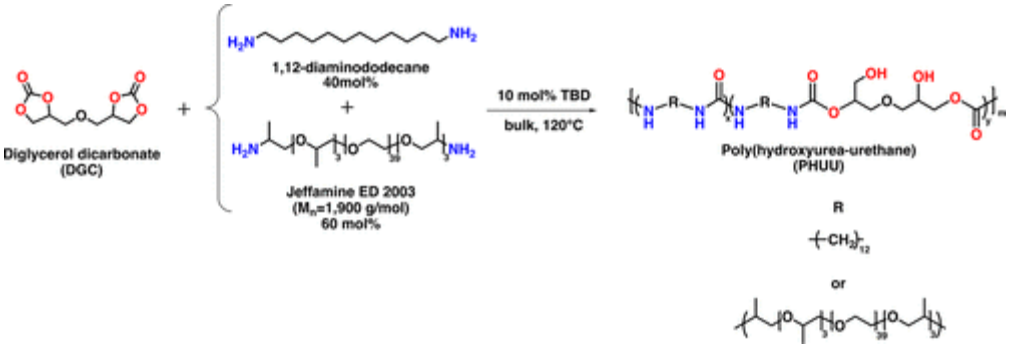

Scheme 3. Synthesis of Poly(hydroxyurea–urethane)s (PHUUs) from DGC and Diamines at 120°C Using 10 mol % of TBD as Catalyst

Analysis by ^{13}C NMR of the carbonyl region expected the presence of two types of urethane groups, namely, one due to Jeffamine ED-2003 (155.6 and 155.3 ppm) and the other one due to 1,12-diaminododecane (156.3 and 155.9 ppm), confirming the successful polymerization. Moreover, three different urea-type (−NH–(C═O)–NH−) carbonyl groups could be observed at 158.1, 157.5, and 156.9 ppm. As the urea content increased, peaks due to the urethane carbonyls progressively disappeared (Figure S19).

The molecular weights of the synthesized PHUUs were estimated by SEC (Table1; see also Figure S37). Molecular weights ranged between 4000 and 11 200 g mol^{-1} with dispersities ranging from 1.6 to 1.8, which are typical for the step-growth polyaddition reaction.

DSC measurements of the PHUUs show soft segment glass transition temperatures (T_g) from −33 to −57 °C (Table1 and Figure S39). Increasing the urea content resulted in a decrease of the T_g of the soft segment of the polymer, likely due to a higher phase separation. This effect was more pronounced for samples containing the short diamine, indicating that the introduction of this compound allowed for a reorganization of the hard and soft segments, giving rise to a segmented phase separated structure. Regarding the semicrystalline PEG chains, we observed a small drop in the enthalpy of melting, as urea groups are formed during the polymerization which can be explained considering a change of PEG segments distribution in the polymer matrix.

The thermomechanical properties of the five synthesized PHUUs containing the short diamine were analyzed by rheological measurements in parallel plates geometry. Figure 5 shows the temperature dependence of the storage modulus (*G'*) of the PHUUs. Consistent with the DSC measurements, all polymers show a drop in elastic modulus at around 32 °C, corresponding to the melting temperature of the aliphatic polyether chain (PEG) of Jeffamine ED-2003. As expected for PHUU4, without any urea domain in the hard segment, the material presents a direct transition from the solid state to the liquid state without a significant rubbery plateau, after the melting temperature of the polyether chain is reached. As described by Torkelson and co-workers, this can be explained by the stronger ability of polyhydroxyurethanes rather than polyurethanes to form hydrogen

bonding between the soft and the hard phases, which limits the phase separation and thus leads to a total loss of rubbery plateau domain.(53)

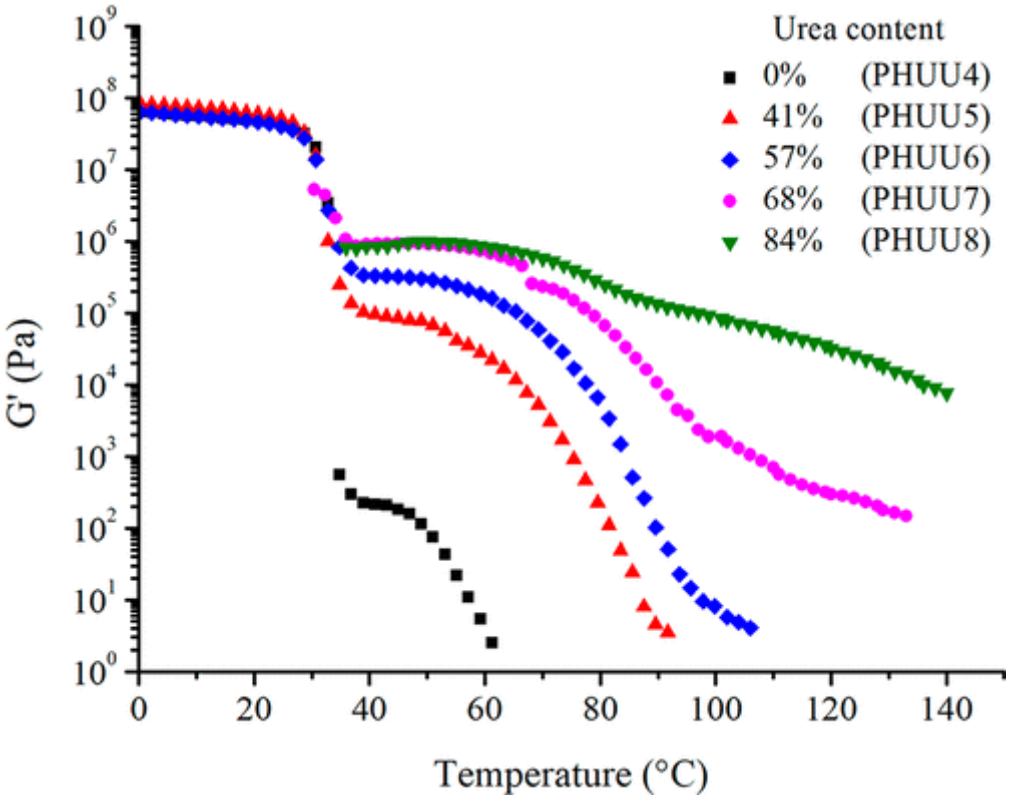

Figure 5. Temperature dependence of storage modulus (*G'*) of the synthesized PHUUs.

Looking at PHUU5, PHUU6, PHUU7, and PHUU8, polymers with urea domains ranging from 41 to 84%, we also observed a drop on *G'* upon heating near the melting temperature of Jeffamine ED-2003. However, in all these cases a rubbery plateau region can be observed that extends to higher temperatures as the urea content is increased.

Figure 6 shows the SAXS curves of the PHUU samples at room temperature and at 60 °C (above the melting temperature of PEG segments). A peak was observed for all the samples at room temperature which vanished at 60 °C. Therefore, these peaks correspond to the long period of the lamellar structure of the matrix phase (PEG), which can be estimated according to $d = 2\pi/q_{max}$ and listed in Table1. The values of long period obtained correspond to the average distance between the crystalline lamellar centers of PEG. When the samples are heated to 60 °C, the long period peaks vanished as PEG melts. For PHUU4, a broad peak was observed at intermediate *q* range and a power law at low *q*. For all of the other samples, only a power law was observed. The general SAXS features are very different from the self-assembly morphology of block copolymers with microphase separation. For this reason, the phase behavior was examined by phase contrast optical microscopy.

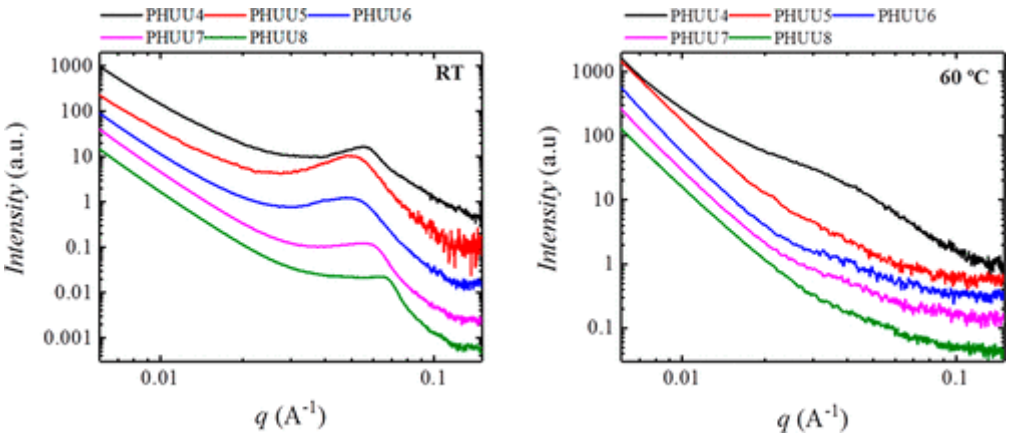

Figure 6. SAXS patterns of the synthesized PHUUs at room temperature and at 60 °C.

Phase contrast optical microscopy images are shown in Figure 7. All PHUU samples exhibit macroscopic phase separation at 40 °C. These results explain the lack of structure detected by SAXS at temperatures above the melting point of the PEG crystals, as the scale of phase segregation is beyond the resolution of the SAXS. The amount of phase-segregated domains increased from PHUU4 to PHUU8. Phase segregation was thus favored by the presence of urea groups. At 80 °C, a uniform phase was obtained for PHUU4.

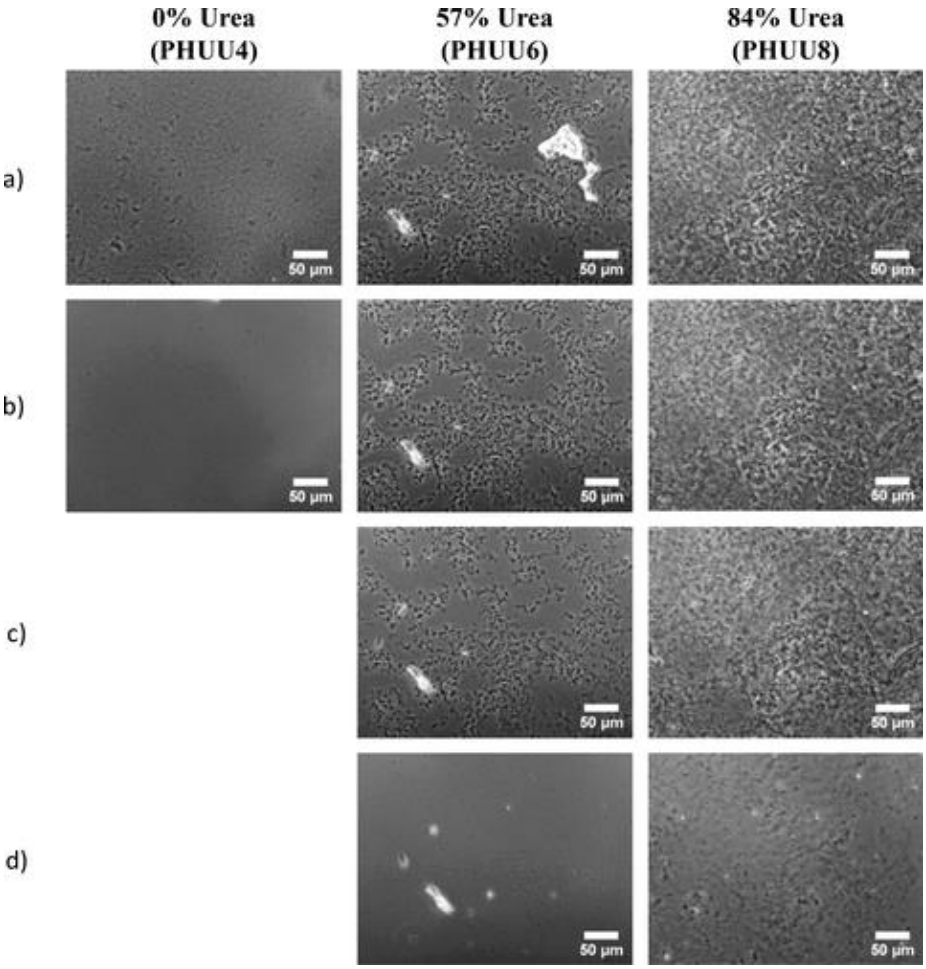

Figure 7. Phase-contrast microscopy images of PHUU4, PHUU6, and PHUU8 at (a) 40, (b) 80, (c) 120, and (d) 200 °C. Note: the phase-contrast microscopy images of PHUU4 at 120 and 200 °C did not show any differences with the one obtained at 80 °C.

On the other hand, at 200 °C, PHUU6 exhibited a single phase while PHUU8 still showed some phase-separated morphology. The miscibility temperatures shown in optical microscopy followed the same trend, as the transition temperature shown by rheology, although the former ones were higher.

Taken together, rheometry, SAXS, and phase contrast microscopy results indicate that the poly(hydroxyurea–urethane)s experience an order–disorder transition at temperatures well above the glass transition temperature of the hard segments. Upon cooling from a single-phase melt, the materials phase segregate as the hard segments vitrified, and further cooling leads to the crystallization of the PEG phase.

Finally, increasing the urea content in the hard segment up to 84% (PHUU8) promoted an elastomeric behavior of the material well above the melting temperature of the Jeffamine polyether chain, as confirmed in the rheology measurement by a rubbery plateau regime up to 140 °C. This effect was attributed to the improved phase separation of soft and hard segments probably due to the presence of lower amounts of pending hydroxyl groups in the hard segment which substantially reduce the ability of PHUUs to form hydrogen bonding with the oxygen of the ether groups of the soft segment. Furthermore, structure–property relationship studies that consider the influence of the hydroxyl group in the phase separation are underway in our laboratory to synthesize segmented PHUUs with improved properties.

4. Conclusion

A new synthetic approach to poly(hydroxyurea–urethane)s in a one-pot process following an organocatalytic pathway starting from a five-membered dicyclic carbonate and a diamine has been developed. The polymerization reaction outcomes are highly catalyst dependent. During the polymerization between diglycerol dicarbonate and diamines, some side-reactions may take place favoring the formation of ureas. Our findings suggest that these side-reactions are more pronounced when using strong base catalysts such as TBD or P_4. In order to get a better understanding of the urea formation, a model reaction between propylene carbonate and dodecylamine was performed showing that with strong bases such as TBD and by increasing the temperature mainly urea could be formed from cyclic carbonates. A mechanism has been proposed to explain the formation of urea from urethane after completion of the reaction. Taking advantage of this reaction, we synthesized different PHUUs with controlled urethane-to-urea ratio. We found that increasing the urea content led to phase separation in poly(hydroxyurea–urethane) even in the presence of polyether-based soft segments. Together, these results confirm that when using base catalysts, it is possible to synthesize isocyanate-free poly(hydroxyurea–urethane) in one pot and to obtain phase-separated poly(hydroxyurea–urethane)s using conventional polyether-based soft segments.

Acknowledgments

The authors thank the European Commission for its financial support through the projects SUSPOL-EJD 642671, Renaissance-ITN 289347, and OrgBIO-ITN 607896. Haritz Sardon gratefully acknowledges financial support from MINECO through project SUSPOL and FDI 16507. A. J. Müller, G. Liu, and H. Sardon also acknowledge European funding by the RISE BIODEST project (H2020-MSCA-RISE-2017-778092). G. Liu is grateful to the support from the Youth Innovation Promotion Association of CAS (2015026). The authors also thank the technical and human support provided by Dr. Patricia Navarro (SGIker) of UPV/EHU and European funding (ERDF and ESF) for the mass spectra analysis and Mrs. Sofia Guezala (SGIker) of UPV/EHU for the ^{13}C NMR analysis.

References

1. Kathalewar, M. S.; Joshi, P. B.; Sabnis, A. S.; Malshe, V. C. Non-Isocyanate Polyurethanes: From Chemistry to Applications. *RSC Adv.* **2013**, *3* (13), 4110– 4129, DOI: 10.1039/c2ra21938g
2. Blattmann, H.; Fleischer, M.; Bähr, M.; Mülhaupt, R. Isocyanate- and Phosgene-Free Routes to Polyfunctional Cyclic Carbonates and Green Polyurethanes by Fixation of Carbon Dioxide. *Macromol. Rapid Commun.* **2014**, *35* (14), 1238– 1254, DOI: 10.1002/marc.201400209
3. Besse, V.; Camara, F.; Voirin, C.; Auvergne, R.; Caillol, S.; Boutevin, B. Synthesis and Applications of Unsaturated Cyclocarbonates. *Polym. Chem.* **2013**, *4* (17), 4545– 4561, DOI: 10.1039/c3py00343d
4. Rokicki, G.; Parzuchowski, P. G.; Mazurek, M. Non-Isocyanate Polyurethanes: Synthesis, Properties, and Applications. *Polym. Adv. Technol.* **2015**, *26* (7), 707– 761, DOI: 10.1002/pat.3522

5. Maisonneuve, L.; Lamarzelle, O.; Rix, E.; Grau, E.; Cramail, H. Isocyanate-Free Routes to Polyurethanes and Poly(hydroxy Urethane)s. *Chem. Rev.* **2015**, *115* (22), 12407– 12439, DOI: 10.1021/acs.chemrev.5b00355
6. Sardon, H.; Pascual, A.; Mecerreyes, D.; Taton, D.; Cramail, H.; Hedrick, J. L. Synthesis of Polyurethanes Using Organocatalysis: A Perspective. *Macromolecules* **2015**, *48* (10), 3153– 3165, DOI: 10.1021/acs.macromol.5b00384
7. Sardon, H.; Engler, A. C.; Chan, J. M. W.; Coady, D. J.; O'Brien, J. M.; Mecerreyes, D.; Yang, Y. Y.; Hedrick, J. L. Homogeneous Isocyanate- and Catalyst-Free Synthesis of Polyurethanes in Aqueous Media. *Green Chem.* **2013**, *15* (5), 1121– 1126, DOI: 10.1039/c3gc40319j
8. Guan, J.; Song, Y.; Lin, Y.; Yin, X.; Zuo, M.; Zhao, Y.; Tao, X.; Zheng, Q. Progress in Study of Non-Isocyanate Polyurethane. *Ind. Eng. Chem. Res.* **2011**, *50* (11), 6517– 6527, DOI: 10.1021/ie101995j
9. Delebecq, E.; Pascault, J.-P.; Boutevin, B.; Ganachaud, F. On the Versatility of Urethane/Urea Bonds: Reversibility, Blocked Isocyanate, and Non-Isocyanate Polyurethane. *Chem. Rev.* **2013**, *113* (1), 80– 118, DOI: 10.1021/cr300195n
10. Lambeth, R. H.; Henderson, T. J. Organocatalytic Synthesis of (poly)hydroxyurethanes from Cyclic Carbonates and Amines. *Polymer* **2013**, *54* (21), 5568– 5573, DOI: 10.1016/j.polymer.2013.08.053
11. Ochiai, B.; Kojima, H.; Endo, T. Synthesis and Properties of Polyhydroxyurethane Bearing Silicone Backbone. *J. Polym. Sci., Part A: Polym. Chem.* **2014**, *52* (8), 1113– 1118, DOI: 10.1002/pola.27091
12. Matsukizono, H.; Endo, T. Synthesis of Polyhydroxyurethanes from Di(trimethylolpropane) and Their Application to Quaternary Ammonium Chloride-Functionalized Films. *RSC Adv.* **2015**, *5* (87), 71360– 71369, DOI: 10.1039/C5RA09885H
13. Tomita, H.; Sanda, F.; Endo, T. Structural Analysis of Polyhydroxyurethane Obtained by Polyaddition of Bifunctional Five-Membered Cyclic Carbonate and Diamine Based on the Model Reaction. *J. Polym. Sci., Part A: Polym. Chem.* **2001**, *39* (6), 851– 859, DOI: 10.1002/1099-0518(20010315)39:6<851::AID-POLA1058>3.0.CO;2-3
14. Ochiai, B.; Satoh, Y.; Endo, T. Nucleophilic Polyaddition in Water Based on Chemo-Selective Reaction of Cyclic Carbonate with Amine. *Green Chem.* **2005**, *7* (11), 765– 767, DOI: 10.1039/b511019j
15. Ochiai, B.; Matsuki, M.; Miyagawa, T.; Nagai, D.; Endo, T. Kinetic and Computational Studies on Aminolysis of Bicyclic Carbonates Bearing Alicyclic Structure Giving Alicyclic Hydroxyurethanes. *Tetrahedron* **2005**, *61* (7), 1835– 1838, DOI: 10.1016/j.tet.2004.12.014
16. Lamarzelle, O.; Durand, P.-L.; Wirotius, A.-L.; Chollet, G.; Grau, E.; Cramail, H. Activated Lipidic Cyclic Carbonates for Non-Isocyanate Polyurethane Synthesis. *Polym. Chem.* **2016**, *7* (7), 1439– 1451, DOI: 10.1039/C5PY01964H
17. Fortman, D. J.; Brutman, J. P.; Cramer, C. J.; Hillmyer, M. A.; Dichtel, W. R. Mechanically Activated, Catalyst-Free Polyhydroxyurethane Vitrimers. *J. Am. Chem. Soc.* **2015**, *137* (44), 14019– 14022, DOI: 10.1021/jacs.5b08084
18. Tomita, H.; Sanda, F.; Endo, T. Polyaddition Behavior of Bis(five- and Six-Membered Cyclic Carbonate)s with Diamine. *J. Polym. Sci., Part A: Polym. Chem.* **2001**, *39* (6), 860– 867, DOI: 10.1002/1099-0518(20010315)39:6<860::AID-POLA1059>3.0.CO;2-2
19. Tomita, H.; Sanda, F.; Endo, T. Reactivity Comparison of Five- and Six-Membered Cyclic Carbonates with Amines: Basic Evaluation for Synthesis of Poly(hydroxyurethane). *J. Polym. Sci., Part A: Polym. Chem.* **2001**, *39* (1), 162– 168, DOI: 10.1002/1099-0518(20010101)39:1<162::AID-POLA180>3.0.CO;2-O
20. Maisonneuve, L.; More, A. S.; Foltran, S.; Alfos, C.; Robert, F.; Landais, Y.; Tassaing, T.; Grau, E.; Cramail, H. Novel Green Fatty Acid-Based Bis-Cyclic Carbonates for the Synthesis of Isocyanate-Free Poly(hydroxyurethane Amide)s. *RSC Adv.* **2014**, *4* (49), 25795– 25803, DOI: 10.1039/C4RA03675A
21. Sanders, D. P.; Fukushima, K.; Coady, D. J.; Nelson, A.; Fujiwara, M.; Yasumoto, M.; Hedrick, J. L. A Simple and Efficient Synthesis of Functionalized Cyclic Carbonate Monomers Using a Versatile Pentafluorophenyl Ester Intermediate. *J. Am. Chem. Soc.* **2010**, *132* (42), 14724– 14726, DOI: 10.1021/ja105332k
22. Al-Azemi, T. F.; Bisht, K. S. Synthesis of Novel Bis- and Tris-(cyclic Carbonate)s and Their Use in Preparation of Polymer Networks. *Polymer* **2002**, *43* (8), 2161– 2167, DOI: 10.1016/S0032-3861(02)00010-1
23. Rokicki, G.; Kowalczyk, T.; Glinski, M. Synthesis of Six-Membered Cyclic Carbonate Monomers by Disproportionation of 1,3-Bis(alkoxycarbonyloxy)propanes and Their Polymerization. *Polym. J.* **2000**, *32* (5), 381– 390, DOI: 10.1295/polymj.32.381
24. Du, Y.; Cai, F.; Kong, D.-L.; He, L.-N. Organic Solvent-Free Process for the Synthesis of Propylene Carbonate from Supercritical Carbon Dioxide and Propylene Oxide Catalyzed by Insoluble Ion Exchange Resins. *Green Chem.* **2005**, *7* (7), 518– 523, DOI: 10.1039/b500074b
25. Klaus, S.; Lehenmeier, M. W.; Anderson, C. E.; Rieger, B. Recent Advances in CO_2/epoxide copolymerization—New Strategies and Cooperative Mechanisms. *Coord. Chem. Rev.* **2011**, *255* (13–14), 1460– 1479, DOI: 10.1016/j.ccr.2010.12.002
26. Decortes, A.; Castilla, A. M.; Kleij, A. W. Salen-Complex-Mediated Formation of Cyclic Carbonates by Cycloaddition of CO_2 to Epoxides. *Angew. Chem., Int. Ed.* **2010**, *49* (51), 9822– 9837, DOI: 10.1002/anie.201002087
27. Alvaro, M.; Baleizao, C.; Das, D.; Carbonell, E.; García, H. CO_2 Fixation Using Recoverable Chromium Salen Catalysts: Use of Ionic Liquids as Cosolvent or High-Surface-Area Silicates as Supports. *J. Catal.* **2004**, *228* (1), 254– 258, DOI: 10.1016/j.jcat.2004.08.022
28. Kawanami, H.; Sasaki, A.; Matsui, K.; Ikushima, Y. A Rapid and Effective Synthesis of Propylene Carbonate Using a Supercritical CO_2–ionic Liquid System. *Chem. Commun.* **2003**, *7*, 896– 897, DOI: 10.1039/b212823c
29. Chatelet, B.; Joucla, L.; Dutasta, J.-P.; Martinez, A.; Szeto, K. C.; Dufaud, V. Azaphosphatranes as Structurally Tunable Organocatalysts for Carbonate Synthesis from CO_2 and Epoxides. *J. Am. Chem. Soc.* **2013**, *135* (14), 5348– 5351, DOI: 10.1021/ja402053d
30. Fiorani, G.; Guo, W.; Kleij, A. W. Sustainable Conversion of Carbon Dioxide: The Advent of Organocatalysis. *Green Chem.* **2015**, *17* (3), 1375– 1389, DOI: 10.1039/C4GC01959H
31. Alves, M.; Grignard, B.; Mereau, R.; Jerome, C.; Tassaing, T.; Detrembleur, C. Organocatalyzed Coupling of Carbon Dioxide with Epoxides for the Synthesis of Cyclic Carbonates: Catalyst Design and Mechanistic Studies. *Catal. Sci. Technol.* **2017**, *7* (13), 2651– 2684, DOI: 10.1039/C7CY00438A
32. Cornille, A.; Auvergne, R.; Figovsky, O.; Boutevin, B.; Caillol, S. A Perspective Approach to Sustainable Routes for Non-Isocyanate Polyurethanes. *Eur. Polym. J.* **2017**, *87*, 535– 552, DOI: 10.1016/j.eurpolymj.2016.11.027
33. Gennen, S.; Grignard, B.; Tassaing, T.; Jérôme, C.; Detrembleur, C. CO_2-Sourced α-Alkylidene Cyclic Carbonates: A Step Forward in the Quest for Functional Regioregular Poly(urethane)s and Poly(carbonate)s. *Angew. Chem., Int. Ed.* **2017**, *56* (35), 10394– 10398, DOI: 10.1002/anie.201704467
34. Cornille, A.; Blain, M.; Auvergne, R.; Andrioletti, B.; Boutevin, B.; Caillol, S. Study of Cyclic Carbonate Aminolysis at Room Temperature: Effect of Cyclic Carbonates Structure and Solvent on Polyhydroxyurethane Synthesis. *Polym. Chem.* **2017**, *8*, 592– 604, DOI: 10.1039/C6PY01854H
35. Yamazaki, E.; Hanahata, H.; Hiwatari, J.; Kitahama, Y. Segmented Poly(urethane-Urea)s Synthesized Directly from Isocyanate-Terminated Prepolymers and Masked Diamines I. Quantitative Synthesis. *Polym. J.* **1997**, *29* (10), 811– 817, DOI: 10.1295/polymj.29.811
36. Szycher, M. *Szycher's Handbook of Polyurethanes*, 1st ed.; CRC Press: **1999**.

37. Coleman, M. M.; Skrovanek, D. J.; Hu, J.; Painter, P. C. Hydrogen Bonding in Polymer Blends. 1. FTIR Studies of Urethane-Ether Blends. *Macromolecules* **1988**, *21* (1), 59– 65, DOI: 10.1021/ma00179a014
38. Li, S.; Zhao, J.; Zhang, Z.; Zhang, J.; Yang, W. Aliphatic Thermoplastic Polyurethane-Ureas and Polyureas Synthesized through a Non-Isocyanate Route. *RSC Adv.* **2015**, *5* (9), 6843– 6852, DOI: 10.1039/C4RA12195C
39. Tang, D.; Mulder, D.-J.; Noordover, B. A. J.; Koning, C. E. Well-Defined Biobased Segmented Polyureas Synthesis via a TBD-Catalyzed Isocyanate-Free Route. *Macromol. Rapid Commun.* **2011**, *32* (17), 1379– 1385, DOI: 10.1002/marc.201100223
40. Ma, S.; Liu, C.; Sablong, R. J.; Noordover, B. A. J.; Hensen, E. J. M.; van Benthem, R. A. T. M.; Koning, C. E. Catalysts for Isocyanate-Free Polyurea Synthesis: Mechanism and Application. *ACS Catal.* **2016**, *6* (10), 6883– 6891, DOI: 10.1021/acscatal.6b01673
41. van Velthoven, J. L. J.; Gootjes, L.; van Es, D. S.; Noordover, B. A. J.; Meuldijk, J. Poly(hydroxy Urethane)s Based on Renewable Diglycerol Dicarbonate. *Eur. Polym. J.* **2015**, *70*, 125– 135, DOI: 10.1016/j.eurpolymj.2015.07.011
42. Tryznowski, M.; Świderska, A.; Żołek-Tryznowska, Z.; Gołofit, T.; Parzuchowski, P. G. Facile Route to Multigram Synthesis of Environmentally Friendly Non-Isocyanate Polyurethanes. *Polymer* **2015**, *80*, 228– 236, DOI: 10.1016/j.polymer.2015.10.055
43. Tryznowski, M.; Świderska, A.; Żołek-Tryznowska, Z.; Gołofit, T.; Parzuchowski, P. G. Data on Synthesis and Characterization of New Diglycerol Based Environmentally Friendly Non-Isocyanate Poly(hydroxyurethanes). *Data Brief* **2016**, *6*, 77– 82, DOI: 10.1016/j.dib.2015.11.034
44. Blain, M.; Jean-Gérard, L.; Auvergne, R.; Benazet, D.; Caillol, S.; Andrioletti, B. Rational Investigations in the Ring Opening of Cyclic Carbonates by Amines. *Green Chem.* **2014**, *16* (9), 4286– 4291, DOI: 10.1039/C4GC01032A
45. Zhang, X.; Jones, G. O.; Hedrick, J. L.; Waymouth, R. M. Fast and Selective Ring-Opening Polymerizations by Alkoxides and Thioureas. *Nat. Chem.* **2016**, *8* (11), 1047– 1053, DOI: 10.1038/nchem.2574
46. Lin, B.; Waymouth, R. M. Urea Anions: Simple, Fast, and Selective Catalysts for Ring-Opening Polymerizations. *J. Am. Chem. Soc.* **2017**, *139* (4), 1645– 1652, DOI: 10.1021/jacs.6b11864
47. Dove, A. P. Controlled Ring-Opening Polymerisation of Cyclic Esters: Polymer Blocks in Self-Assembled Nanostructures. *Chem. Commun.* **2008**, *48*, 6446– 6470, DOI: 10.1039/b813059k
48. Pratt, R. C.; Lohmeijer, B. G. G.; Long, D. A.; Waymouth, R. M.; Hedrick, J. L. Triazabicyclodecene: A Simple Bifunctional Organocatalyst for Acyl Transfer and Ring-Opening Polymerization of Cyclic Esters. *J. Am. Chem. Soc.* **2006**, *128* (14), 4556– 4557, DOI: 10.1021/ja060662+
49. Dove, A. P.; Pratt, R. C.; Lohmeijer, B. G. G.; Waymouth, R. M.; Hedrick, J. L. Thiourea-Based Bifunctional Organocatalysis: Supramolecular Recognition for Living Polymerization. *J. Am. Chem. Soc.* **2005**, *127* (40), 13798– 13799, DOI: 10.1021/ja0543346
50. Chen, X.; Li, L.; Jin, K.; Torkelson, J. M. Reprocessable Polyhydroxyurethane Networks Exhibiting Full Property Recovery and Concurrent Associative and Dissociative Dynamic Chemistry via Transcarbamoylation and Reversible Cyclic Carbonate Aminolysis. *Polym. Chem.* **2017**, *8*, 6349, DOI: 10.1039/C7PY01160A
51. Pyo, S.-H.; Hatti-Kaul, R. Chlorine-Free Synthesis of Organic Alkyl Carbonates and Five- and Six-Membered Cyclic Carbonates. *Adv. Synth. Catal.* **2016**, *358* (5), 834– 839, DOI: 10.1002/adsc.201500654
52. Fortman, D. J.; Brutman, J. P.; Hillmyer, M. A.; Dichtel, W. R. Structural Effects on the Reprocessability and Stress Relaxation of Crosslinked Polyhydroxyurethanes. *J. Appl. Polym. Sci.* **2017**, *134*, 44984, DOI: 10.1002/app.44984
53. Leitsch, E. K.; Beniah, G.; Liu, K.; Lan, T.; Heath, W. H.; Scheidt, K. A.; Torkelson, J. M. Nonisocyanate Thermoplastic Polyhydroxyurethane Elastomers via Cyclic Carbonate Aminolysis: Critical Role of Hydroxyl Groups in Controlling Nanophase Separation. *ACS Macro Lett.* **2016**, *5* (4), 424– 429, DOI: 10.1021/acsmacrolett.6b00102
54. Beniah, G.; Chen, X.; Uno, B. E.; Liu, K.; Leitsch, E. K.; Jeon, J.; Heath, W. H.; Scheidt, K. A.; Torkelson, J. M. Combined Effects of Carbonate and Soft-Segment Molecular Structures on the Nanophase Separation and Properties of Segmented Polyhydroxyurethane. *Macromolecules* **2017**, *50* (8), 3193– 3203, DOI: 10.1021/acs.macromol.6b02513

Electronic Supplementary Information for

Unexpected synthesis of segmented poly(hydroxyurea-urethane)s from dicyclic carbonates and diamines by organocatalysis

Amaury Bossion[†,‡], Roberto H. Aguirresarobe[†], Lourdes Irusta[†], Daniel Taton[‡], [‡], Henri Cramail[‡], Etienne Grau[‡], David Mecerreyes[†,§], Cui Su[∥,⊥], Guoming Liu[∥], Alejandro J. Müller[†,§] and Haritz Sardon[†*]

[†]POLYMAT and Polymer Science and Technology Department, Faculty of Chemistry, University of the Basque Country UPV/EHU, Paseo Manuel de Lardizabal 3, 20018, Donostia-San Sebastián, Spain

[‡]CNRS, Laboratoire de Chimie des Polymères Organiques (LCPO), ENSCBP, 16 Avenue Pey Berland, 33607 Pessac, France

[‡]Université de Bordeaux, Laboratoire de Chimie des Polymères Organiques (LCPO), ENSCBP, 16 Avenue Pey Berland, 33607 Pessac, France

[§]kerbasque, Basque Foundation for Science, E-48011 Bilbao, Spain

[∥]CAS Key Laboratory of Engineering Plastics, CAS Research/Education Center for Excellence in Molecular Sciences, Institute of Chemistry, Chinese Academy of Sciences, Beijing, 100190, P. R. China.

[⊥]University of Chinese Academy of Sciences, Beijing 100049, P. R. China

Content:

Part 1: **^{1}H and ^{13}C NMR spectra**

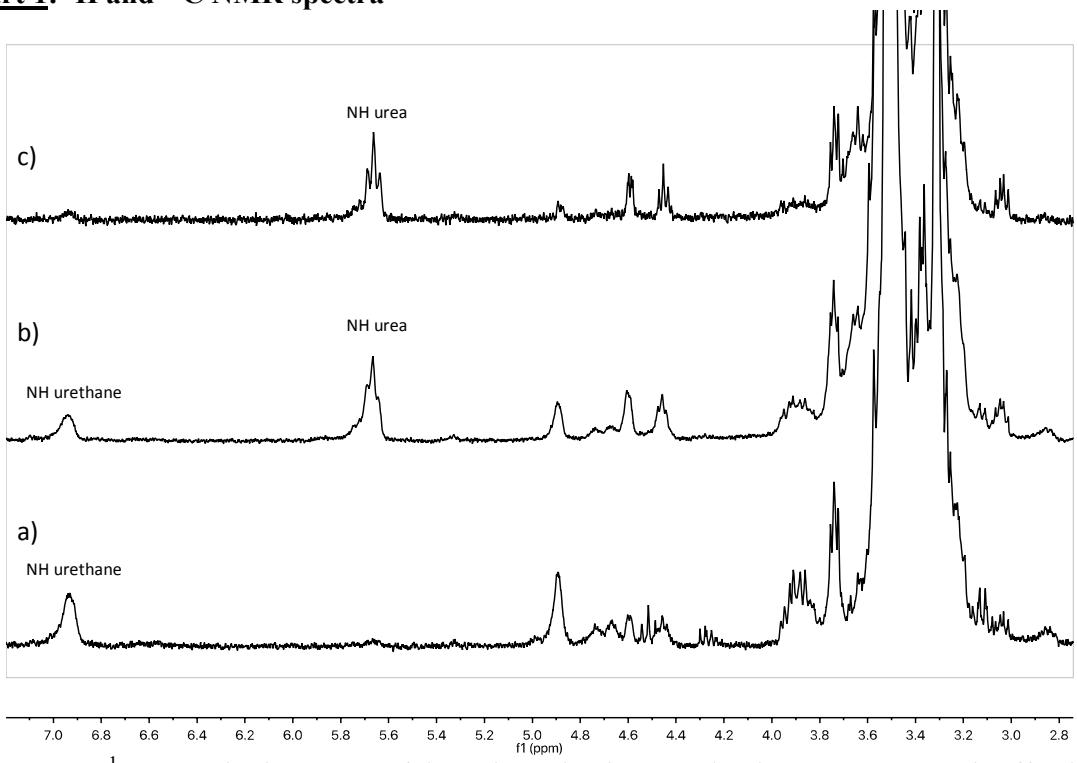

Figure S1. ^{1}H NMR in d_6-DMSO of the polymerization reaction between DGC and Jeffamine ED-2003 at 120°C using TBD as catalyst after a) 1 hour, b) 10 hours and c) 48 hours showing the change in the shifts of the NH protons.

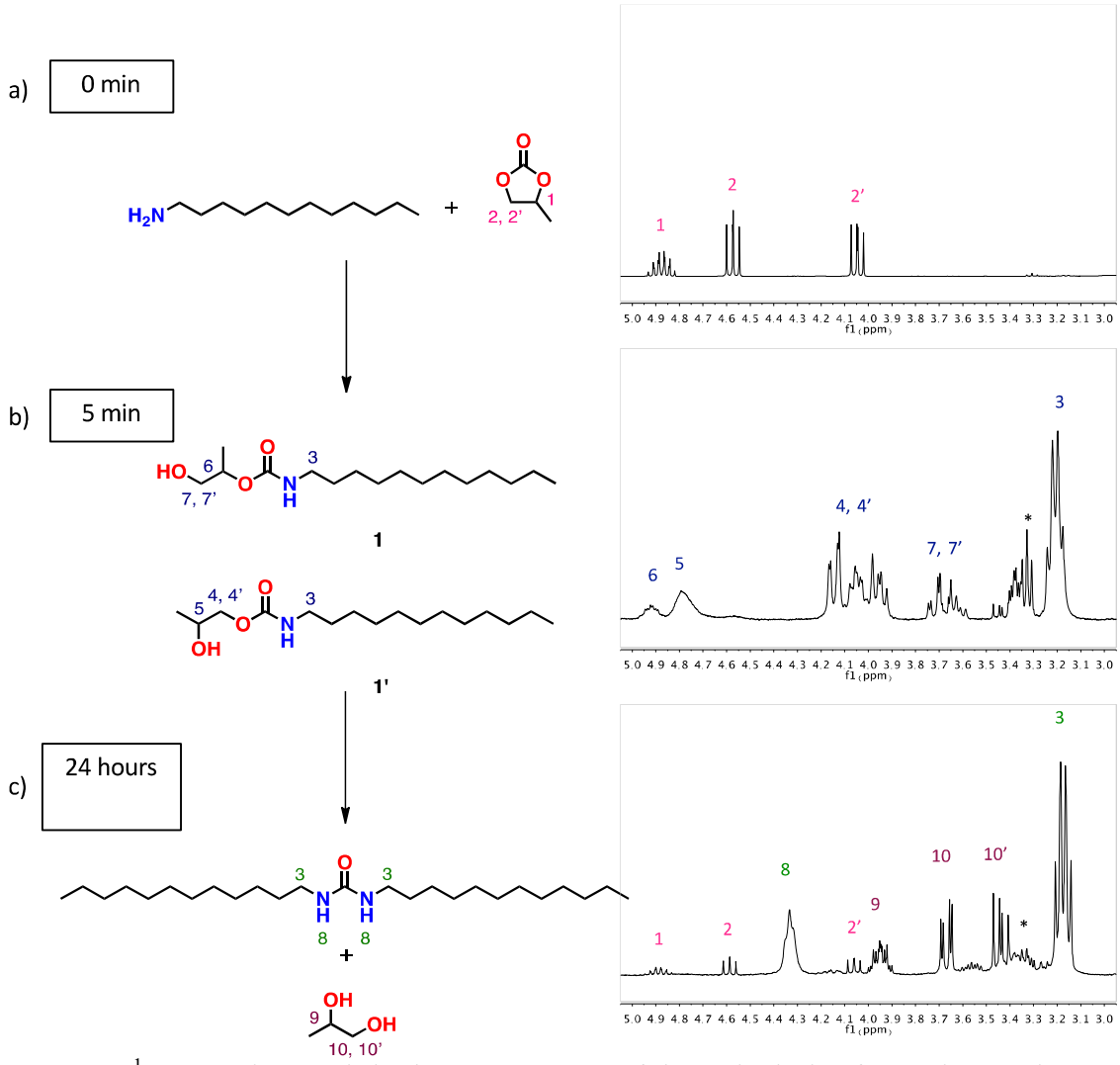

Figure S2. ^{1}H NMR in $CDCl_3$ in the area 3-5 ppm of the aminolysis of propylene carbonate with dodecylamine at 120°C using TBD as catalyst at different reaction time. *(Signal of TBD have been labeled with *).*

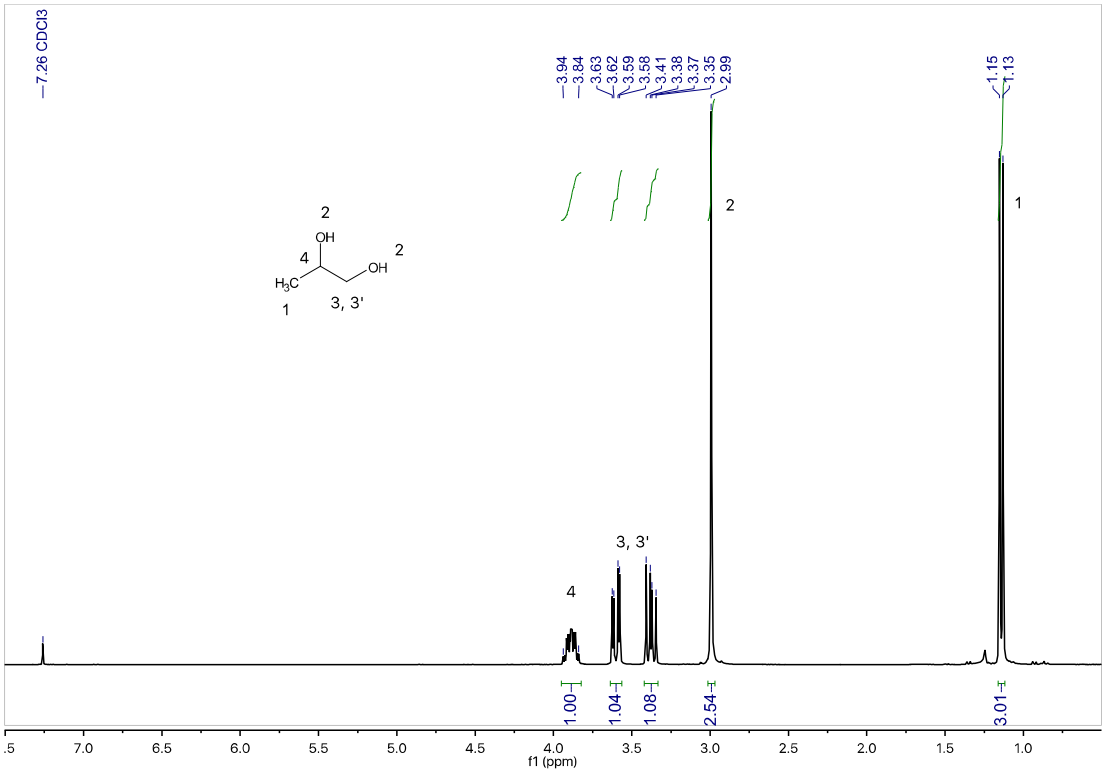

Figure S3. ^{1}H NMR in $CDCl_3$ of the condensate, propane-1,2-diol, that appeared during the aminolysis of propylene carbonate with dodecylamine at 120°C using TBD as catalyst.

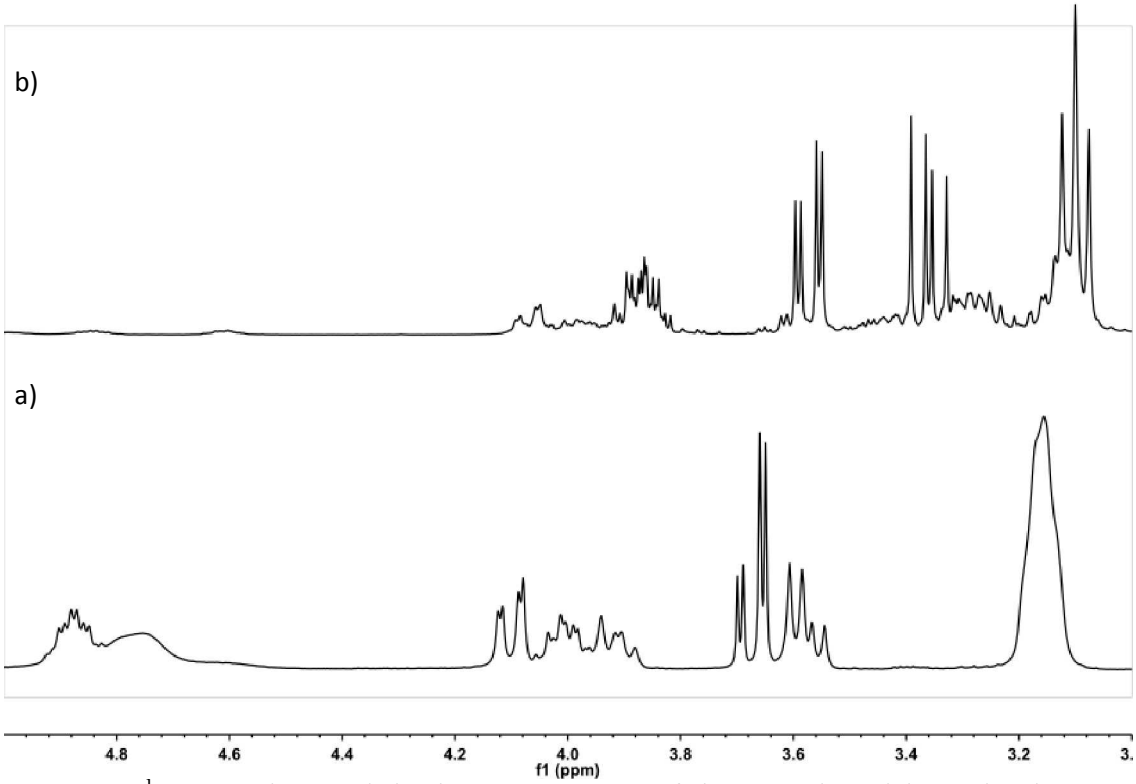

Figure S4. ^{1}H NMR in $CDCl_3$ in the area 3-5 ppm of the control model reaction between propylene carbonate and dodecylamine at 120°C after a) 5 hr without catalyst (until complete conversion of propylene carbonate into urethane) and b) 48 hr after incorporation of TBD as catalyst. The b) NMR shows mainly proton shifts of propane-1,2-diol due to partial solubility of urea in $CDCl_3$.

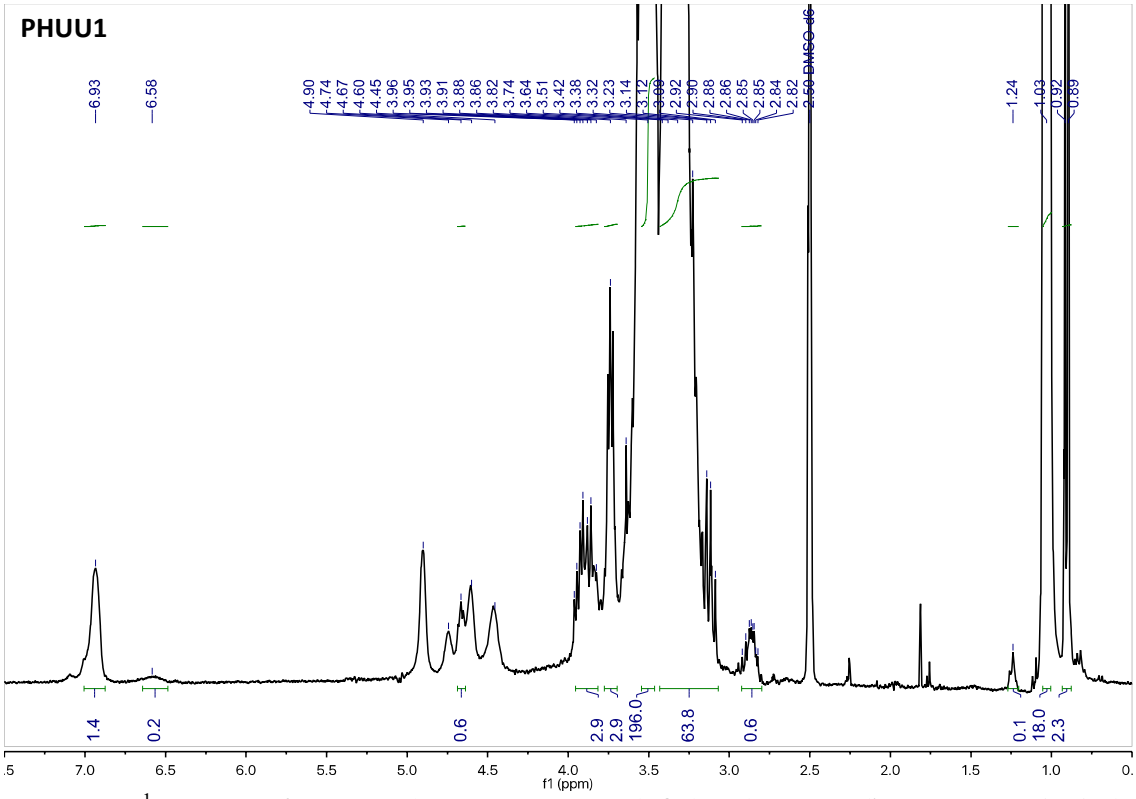

Figure S5. ^{1}H NMR of PHUU1 (300 MHz, DMSO) δ (ppm) = 6.93 (bs, 1.4H, N*H*(CO)O), 6,58 (bs, 0.2H, N*H*(CO)O), 4.90 (bs, *OH*), 4.74 (bs, *OH*), 4.67 (m, 0.6H, C*H*O(CO)N), 3.96-3.82 (m, 2.9H, CH_2OCH_2), 3.74 (m, 2.9H, C*H*OH), 3.64-2.80 (m, 260H, CH_2O and CH_2NH), 1.24 (s, 0.1H, CH_3), 1.03 (m, 18H, CH_3), 0.91-0.89 (m, 2.3H, CH_3). The ratio urethane/urea calculated from the ^{1}H NMR is 100/0.

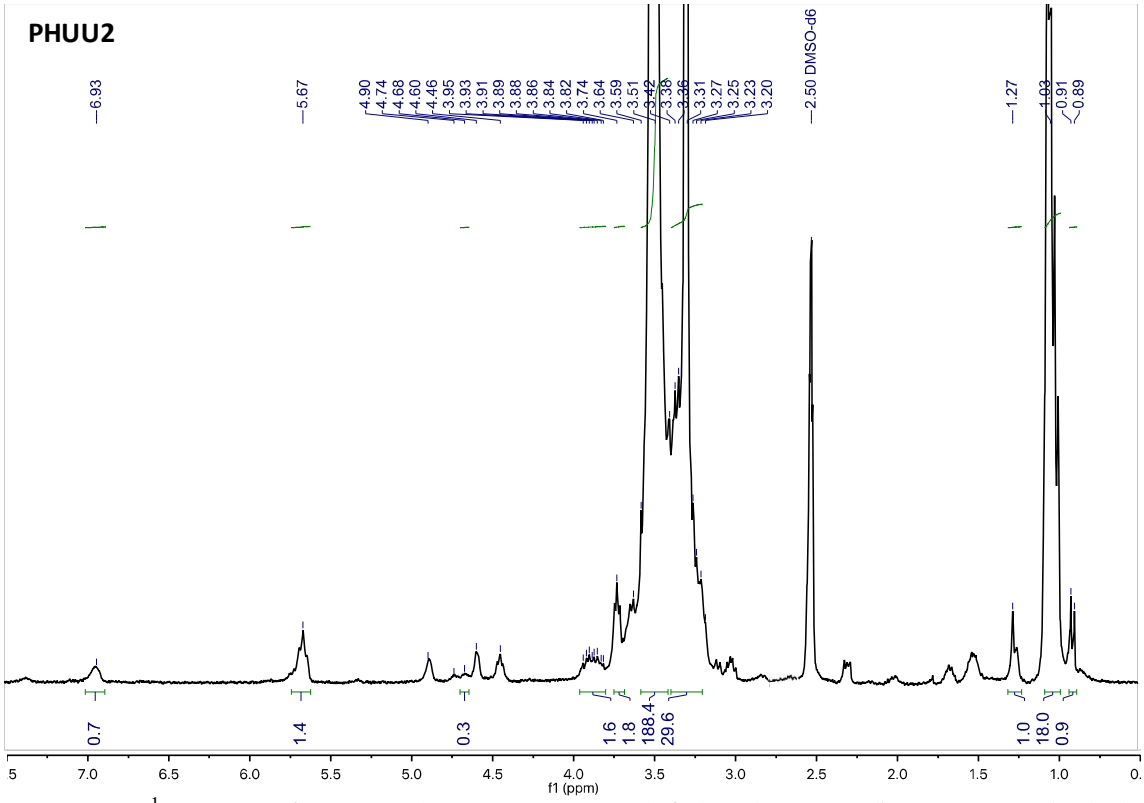

Figure S6. ^{1}H NMR of PHUU2 (300 MHz, DMSO) δ (ppm) = 6.93 (bs, 0.7H, N*H*(CO)O), 5.67 (m, 1.4H, N*H*(CO)N*H*), 4.90 (bs, *OH*), 4.74 (bs, *OH*), 4.68 (m, 0.3H, C*H*O(CO)N), 3.95-3.82 (m, 1.6H, CH_2OCH_2), 3.74 (m, 1.8H, C*H*OH), 3.64-2.80 (m, 218H, CH_2O and CH_2NH), 1.27 (s, 1H, CH_3), 1.03 (m, 18H, CH_3), 0.91-0.89 (m, 0.9H, CH_3). Residual monomer has been labeled with *. The ratio urethane/urea calculated from the ^{1}H NMR is 50/50.

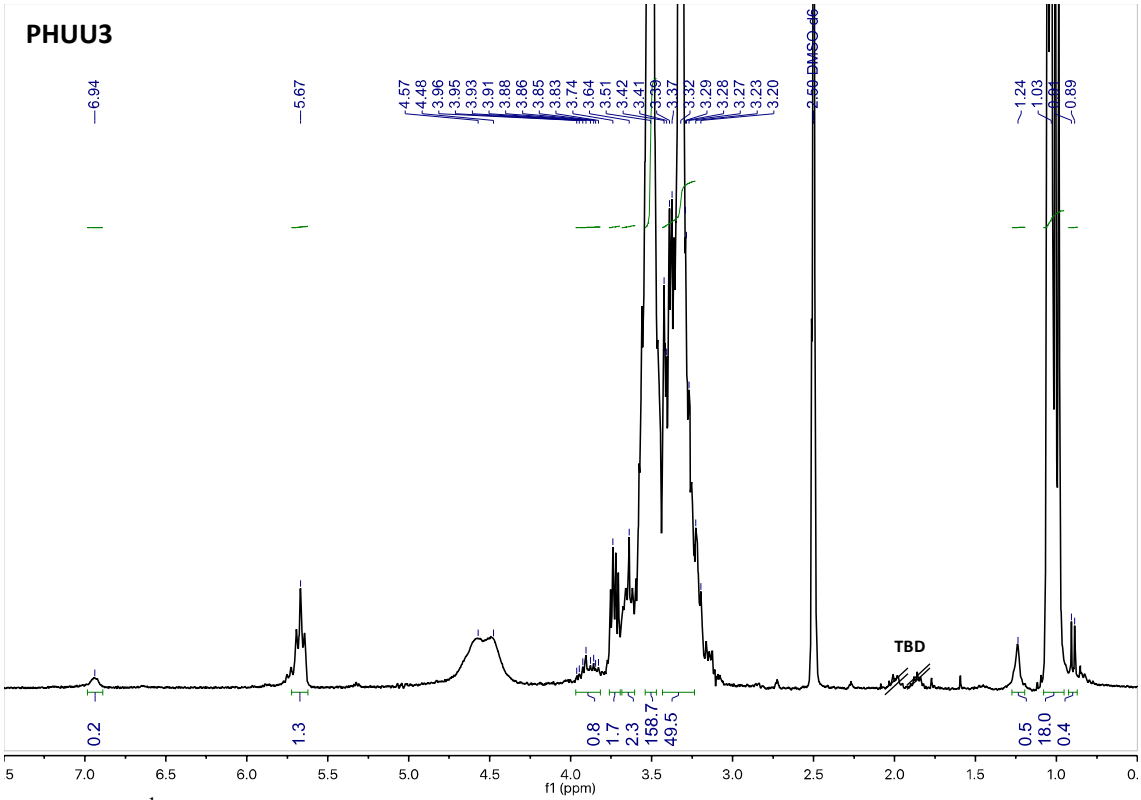

Figure S7. ^{1}H NMR of PHUU3 (300 MHz, DMSO) δ (ppm) = 6.94 (bs, 0.2H, N*H*(CO)O), 5.67 (m, 1.5H, N*H*(CO)N*H*), 4.57-4.48 (bs, *OH* and C*H*O(CO)N), 3.96-3.83 (m, 0.8H, C*H*$_2$OC*H*$_2$), 3.74 (m, 1.7H, C*H*OH), 3.64-3.20 (m, 210H, C*H*$_2$O and C*H*$_2$NH), 1.24 (s, 0.5H, C*H*$_3$), 1.03 (m, 18H, C*H*$_3$), 0.91-0.89 (m, 0.4H, C*H*$_3$). The ratio urethane/urea calculated from the ^{1}H NMR is 23/77.

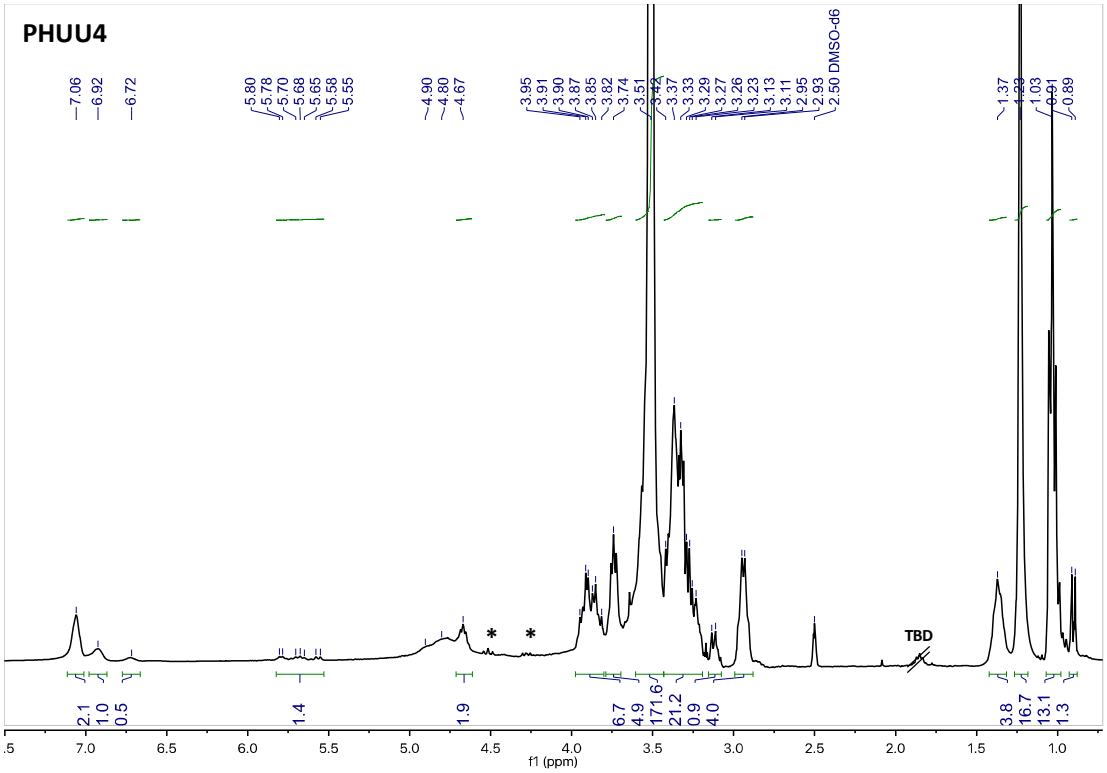

Figure S8. ^{1}H NMR of PHUU4 (300 MHz, DMSO) δ (ppm) = 7.06 (bs, 2.1H, N*H*(CO)O), 6.92 (bs, 1.0H, N*H*(CO)O), 6,72 (bs, 0.5H, N*H*(CO)O), 5.80-5.65 (m, 1.4H, N*H*(CO)N*H*), 4.90 (s, *OH*), 4.80 (s, *OH*), 4.67 (m, 1.9H, C*H*O(CO)N), 3.95-3.82 (m, 6.7H, CH_2OCH_2), 3.74 (m, 4.9H, C*H*OH), 3.51-3.11 (m, 194H, CH_2O), 2.94 (q, 4H, CH_2NH), 1.37 (m, 3.8H, CH_2), 1.23 (s, 16.7H, CH_2), 1.03 (m, 13.1H, CH_3), 0.91-0.89 (m, 1.3H, CH_3). Residual monomer has been labeled with *.

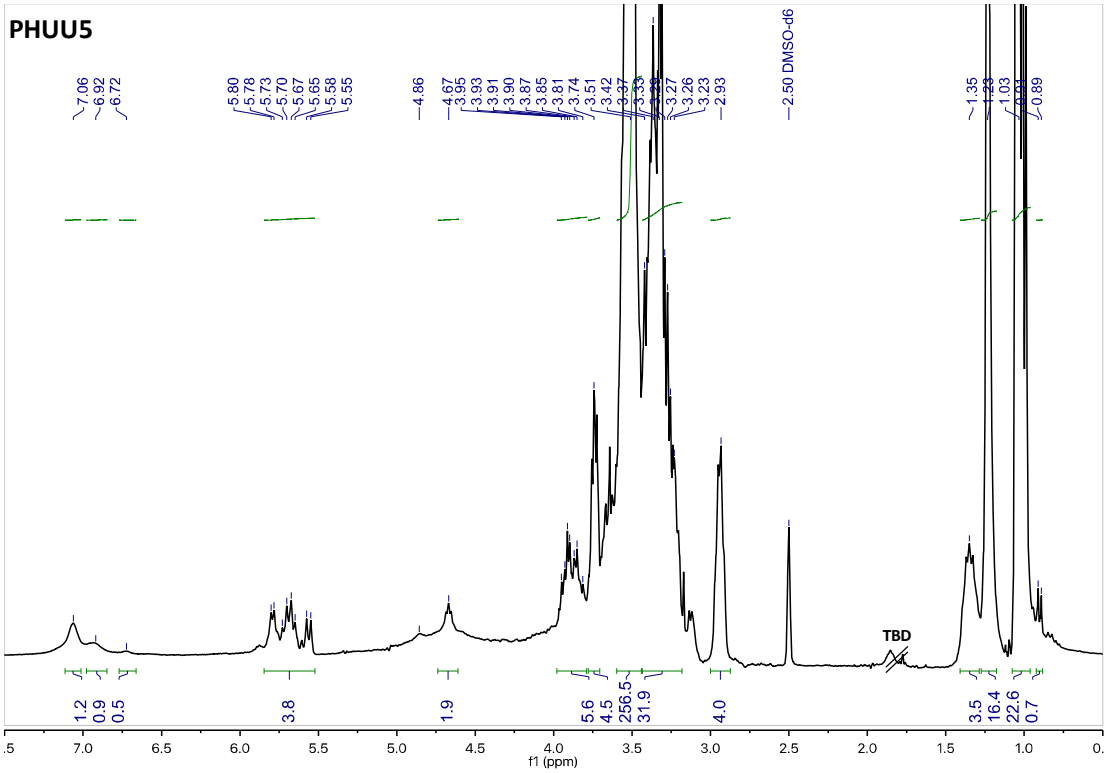

Figure S9. ^{1}H NMR of PHUU5 (300 MHz, DMSO) δ (ppm) = 7.06 (bs, 1.2H, N*H*(CO)O), 6.92 (bs, 0.9H, N*H*(CO)O), 6,72 (bs, 0.5H, N*H*(CO)O), 5.80-5.65 (m, 3.8H, N*H*(CO)N*H*), 4.90 (s, *OH*), 4.80 (s, *OH*), 4.67 (m, 1.9H, C*H*O(CO)N), 3.95-3.82 (m, 5.6H, CH_2OCH_2), 3.74 (m, 4.5H, C*H*OH), 3.51-3.11 (m, 288H, CH_2O), 2.94 (q, 4H, CH_2NH), 1.37 (m, 3.5H, CH_2), 1.23 (s, 16.4H, CH_2), 1.03 (m, 22.6H, CH_3), 0.91-0.89 (m, 0.7H, CH_3). The ratio urethane/urea calculated from the ^{1}H NMR is 58/42.

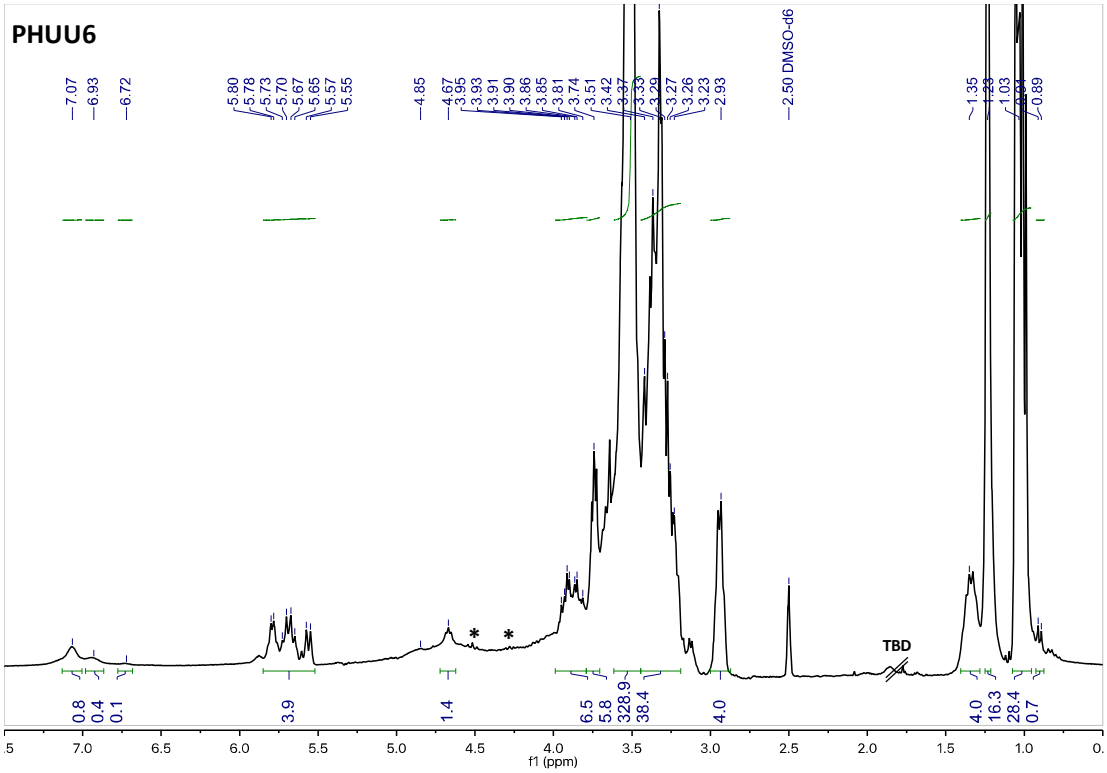

Figure S10. ^{1}H NMR of PHUU6 (300 MHz, DMSO) δ (ppm) = 7.07 (bs, 0.8H, N*H*(CO)O), 6.93 (bs, 0.4H, N*H*(CO)O), 6,72 (bs, 0.1H, N*H*(CO)O), 5.80-5.65 (m, 3.9H, N*H*(CO)N*H*), 4.90 (s, *OH*), 4.80 (s, *OH*), 4.67 (m, 1.4H, C*H*O(CO)N), 3.95-3.82 (m, 6.5H, CH_2OCH_2), 3.74 (m, 5.8H, C*H*OH), 3.51-3.11 (m, 367H, CH_2O), 2.94 (q, 4H, CH_2NH), 1.37 (m, 4H, CH_2), 1.23 (s, 16.3H, CH_2), 1.03 (m, 28.4H, CH_3), 0.91-0.89 (m, 0.7H, CH_3). Residual monomer has been labeled with *. The ratio urethane/urea calculated from the ^{1}H NMR is 40/60.

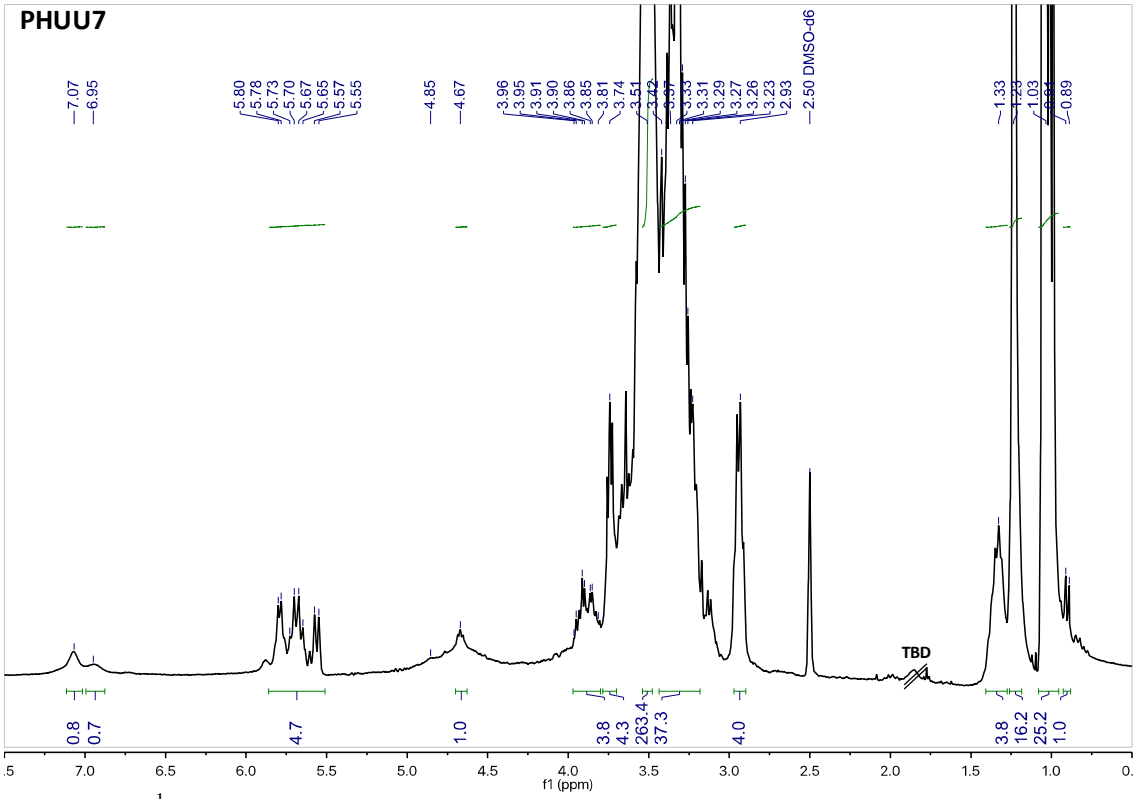

Figure S11. ^{1}H NMR of PHUU7 (300 MHz, DMSO) δ (ppm) = 7.06 (bs, 0.8H, N*H*(CO)O), 6.95 (bs, 0.7H, N*H*(CO)O), 5.80-5.65 (m, 4.7H, N*H*(CO)N*H*), 4.90 (s, *OH*), 4.80 (s, *OH*), 4.67 (m, 1H, C*H*O(CO)N), 3.95-3.82 (m, 3.8H, C*H*$_2$OC*H*$_2$), 3.74 (m, 4.3H, C*H*OH), 3.51-3.11 (m, 300H, C*H*$_2$O), 2.94 (q, 4H, C*H*$_2$NH), 1.37 (m, 3.8H, C*H*$_2$), 1.23 (s, 16.2H, C*H*$_2$), 1.03 (m, 25.2H, C*H*$_3$), 0.91-0.89 (m, 1H, C*H*$_3$). The ratio urethane/urea calculated from the ^{1}H NMR is 39/61.

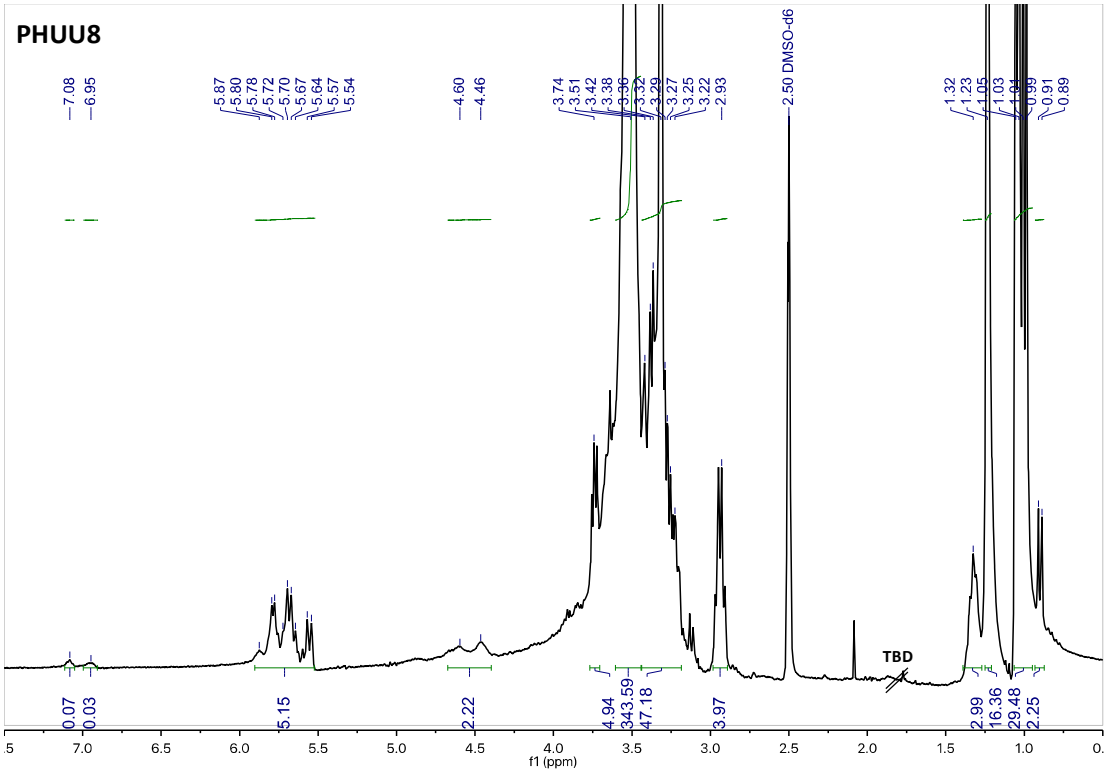

Figure S12. ^{1}H NMR of PHUU8 (300 MHz, DMSO) δ (ppm) = 7.06 (bs, 0.1H, N*H*(CO)O), 6.92 (bs, 0.03H, N*H*(CO)O), 5.80-5.65 (m, 5.2H, N*H*(CO)N*H*), 4.60 (m, 2.2H, C*H*O(CO)N), 3.74 (m, 4.9H, C*H*OH), 3.51-3.11 (m, 391H, CH_2O), 2.94 (q, 4H, CH_2NH), 1.37 (m, 3H, CH_2), 1.23 (s, 16.4H, CH_2), 1.03 (m, 29.5H, CH_3), 0.91-0.89 (m, 2.3H, CH_3). The ratio urethane/urea calculated from the ^{1}H NMR is 5/95.

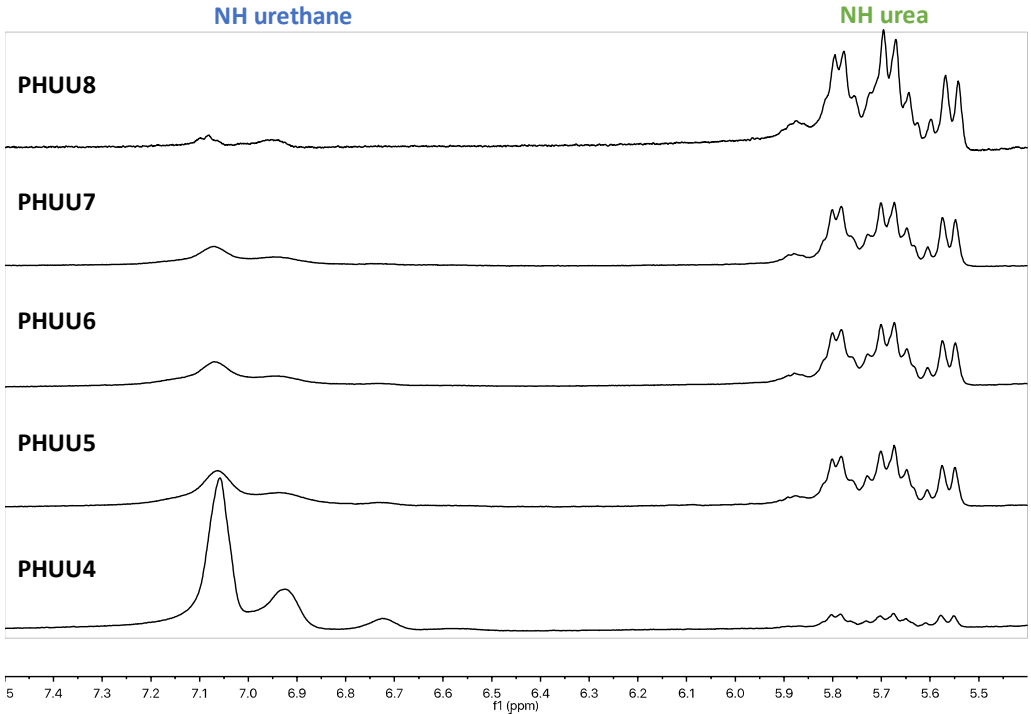

Figure S13. Evolution of the NH bands in the ^{1}H NMR from PHUU4 to PHUU8.

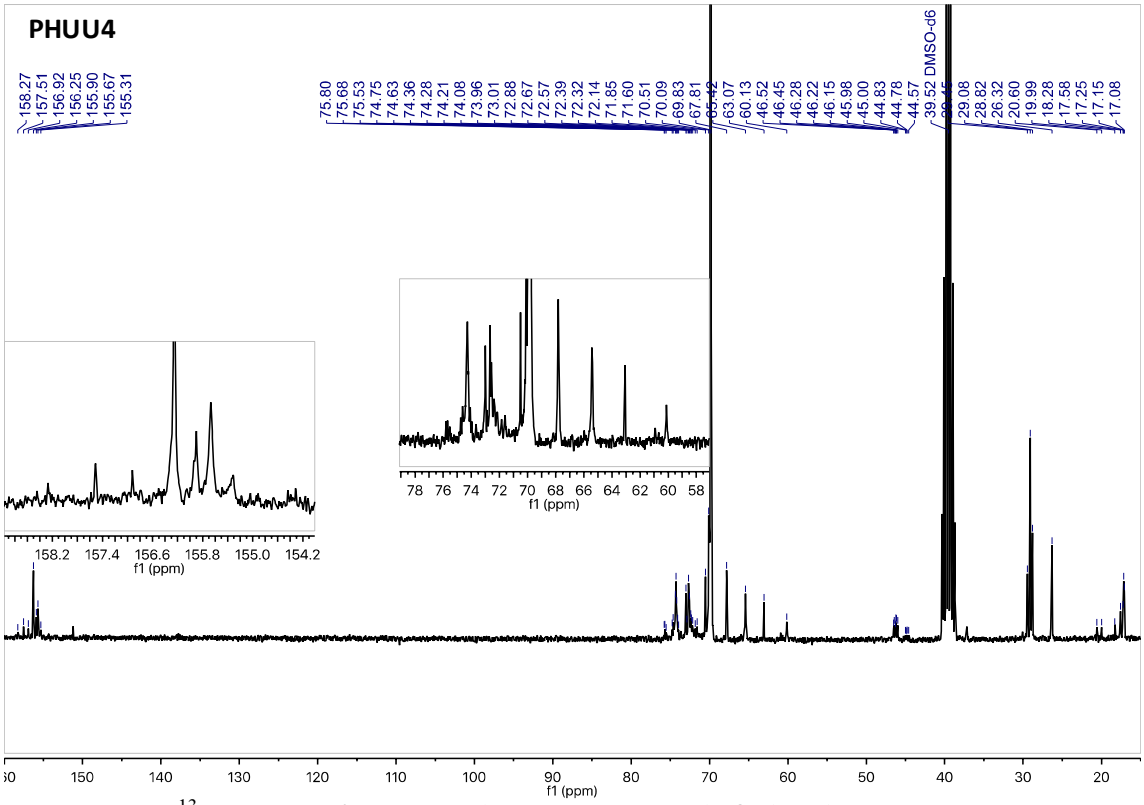

Figure S14. ^{13}C NMR of PHUU4 (75 MHz, DMSO) δ (ppm) = 158.3, 157.5, 156.9 (–NH–(C=O)–NH–), 156.3, 155.9, 155.7, 155.3 (–NH–(C=O)–O–), 75.8, 75.7, 75.5, 74.7-74.0 (m), 73.0-71.6 (m), 70.5, 70.1, 69.8, 67.8, 65.4, 63.1, 60.1 (CH_2O and CHO), 46.5, 46.4, 46.3, 46.2, 46.1, 46.0, 45.0, 44.8, 44.7, 44.6 (CH_2NH), 29.4, 29.1, 28.8, 26.3, 20.6, 19.9, 18.3, 17.6, 17.3, 17.2, 17.1 (CH_3).

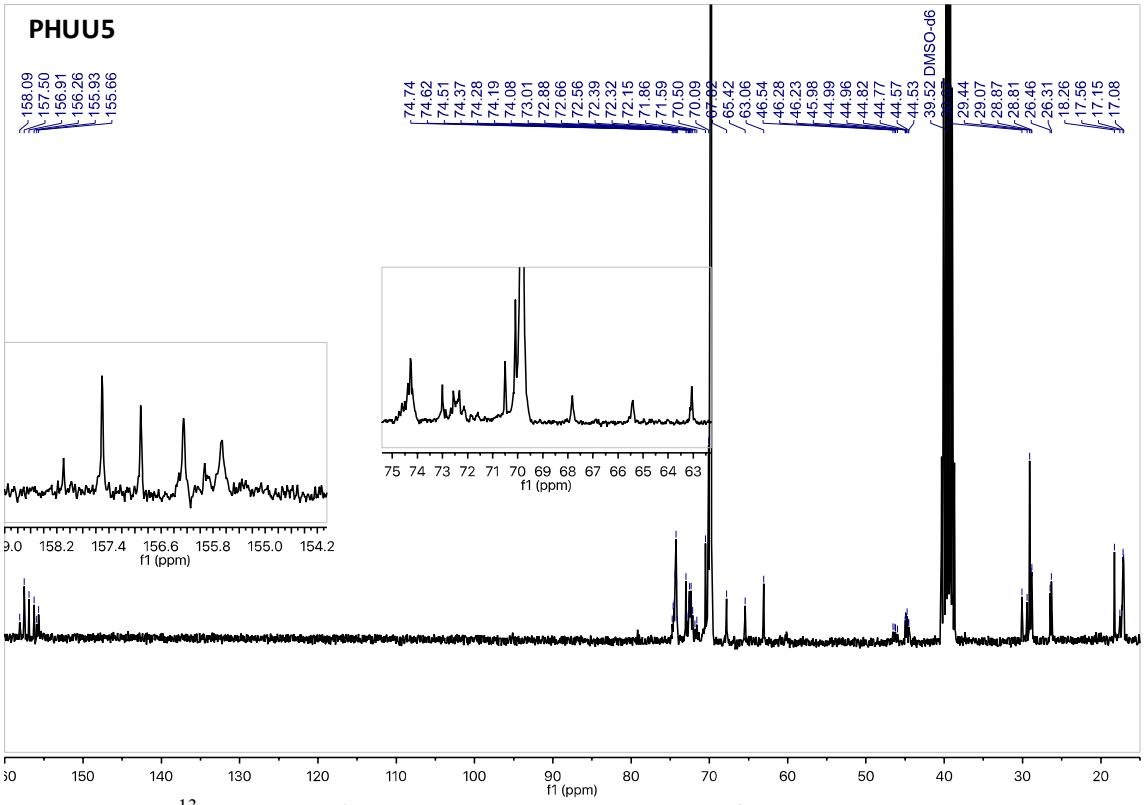

Figure S15. ^{13}C NMR of PHUU5 (75 MHz, DMSO) δ (ppm) = 158.1, 157.5, 156.9 (–NH–(C=O)–NH–), 156.3, 155.9, 155.7 (–NH–(C=O)–O–),74.7-74.0 (m), 73.0-71.6 (m), 70.5, 70.1, 67.8, 65.4, 63.1 (CH_2O and CHO), 46.5, 46.3, 46.2, 46.0, 44.9, 44.8, 44.7, 44.6, 44.5 (CH_2NH), 30.1, 29.4, 29.1, 28.9, 28.8, 26.5, 26.3, 18.3, 17.6, 17.2, 17.1 (CH_3).

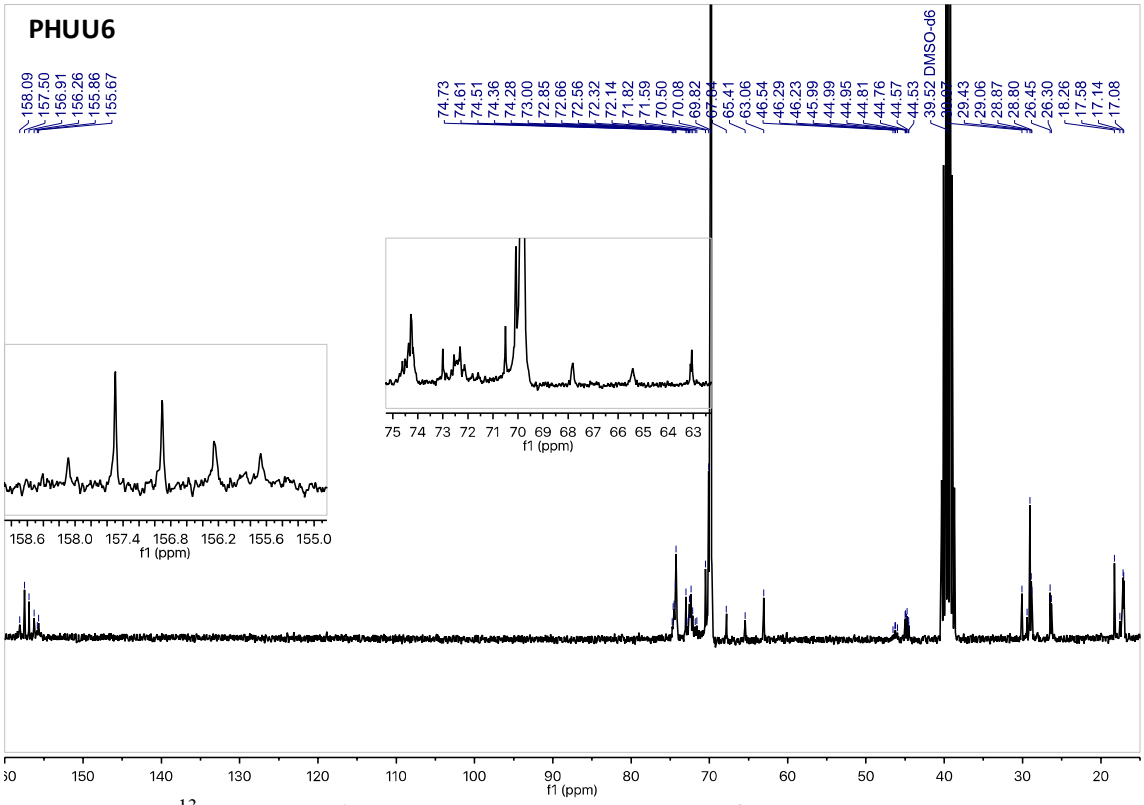

Figure S16. ^{13}C NMR of PHUU6 (75 MHz, DMSO) δ (ppm) = 158.1, 157.5, 156.9 (–NH–(C=O)–NH–), 156.3, 155.9, 155.7 (–NH–(C=O)–O–), 74.7-74.0 (m), 73.0-71.6 (m), 70.5, 70.1, 69.8, 67.8, 65.4, 63.1 (CH_2O and CHO), 46.5, 46.3, 46.2, 46.1, 46.0, 44.9, 44.8, 44.7, 44.6, 44.5 (CH_2NH), 30.1, 20.6, 19.9, 18.3, 17.6, 17.3, 17.2, 17.1 (CH_3).

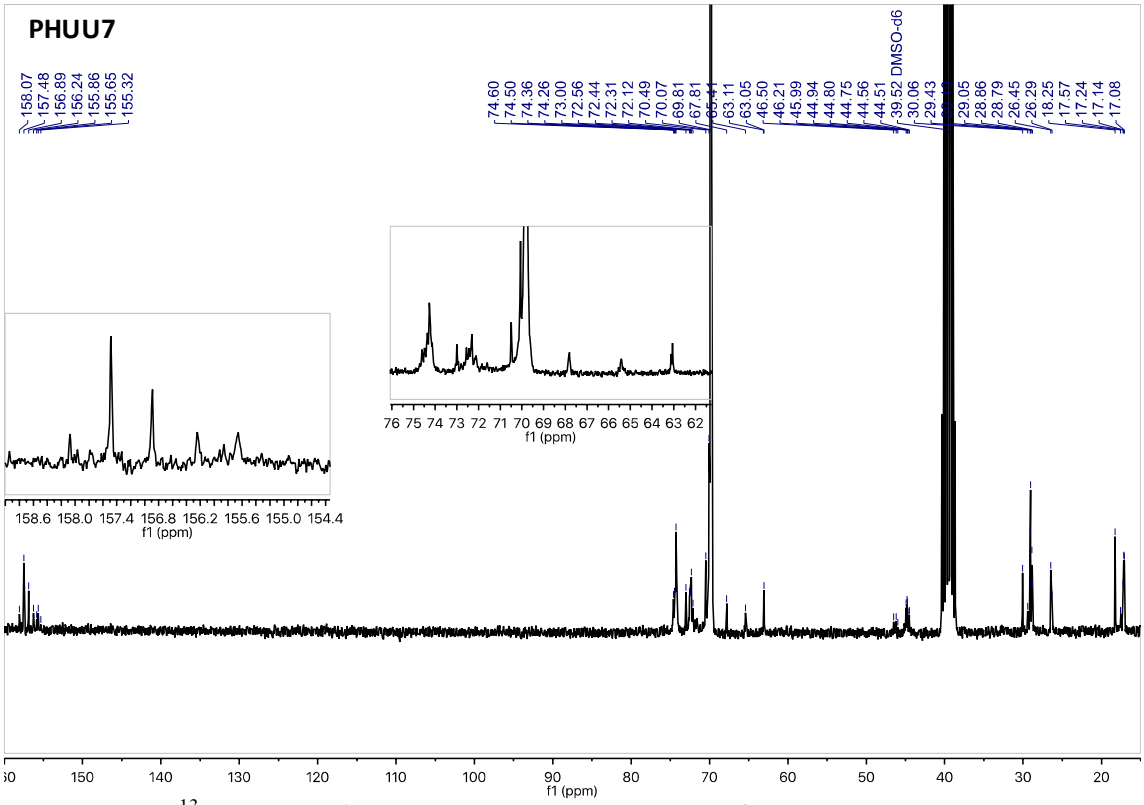

Figure S17. ^{13}C NMR of PHUU7 (75 MHz, DMSO) δ (ppm) = 1581, 157.5, 156.9 (–NH–(C=O)–NH–), 156.3, 155.9, 155.7, 155.3 (–NH–(C=O)–O–), 74.7-74.0 (m), 73.0-71.6 (m), 70.5, 70.1, 69.8, 67.8, 65.4, 63.1 (CH_2O and CHO), 46.5, 46.2, 46.0, 44.9, 44.8, 44.7, 44.6, 44.5 (CH_2NH), 30.1, 29.4, 29.1, 29.0, 28.9, 28.8, 26.5, 26.3, 18.3, 17.6, 17.2, 17.1 (CH_3).

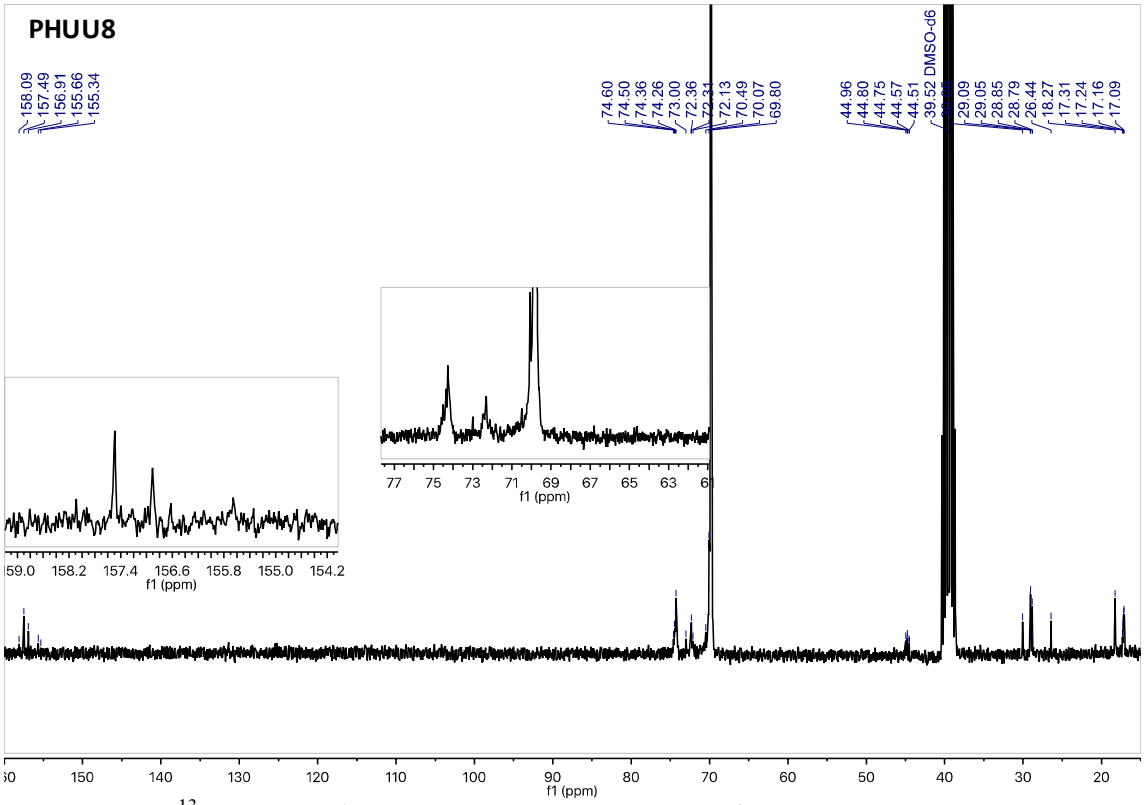

Figure S18. ^{13}C NMR of PHUU8 (75 MHz, DMSO) δ (ppm) = 158.1, 157.5, 156.9 (–NH–(C=O)–NH–), 155.7, 155.3 (–NH–(C=O)–O–), 74.6-74.0 (m), 73.0-72.1 (m), 70.5, 70.1, 69.8 (CH_2O and CHO), 44.9, 44.8, 44.7, 44.6, 44.5 (CH_2NH), 30.1, 29.1, 29.0, 28.9, 28.8, 26.4, 18.3, 17.3, 17.2, 17.1 (CH_3).

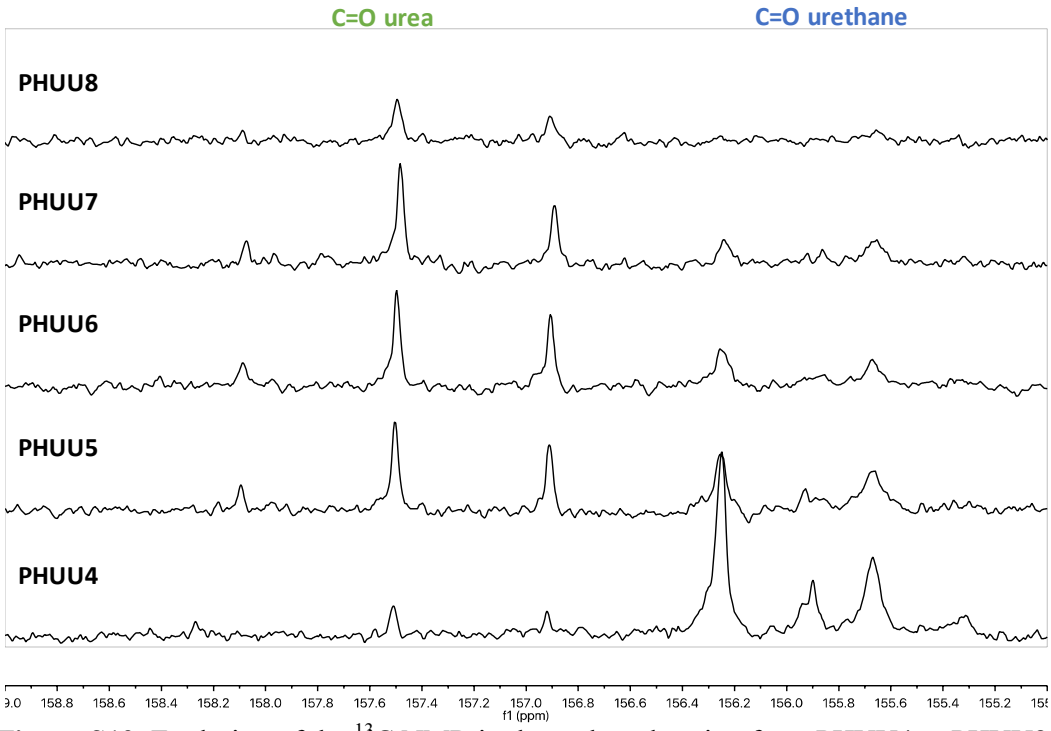

Figure S19. Evolution of the ^{13}C NMR in the carbonyl region from PHUU4 to PHUU8.

Part 2: FTIR-ATR spectra

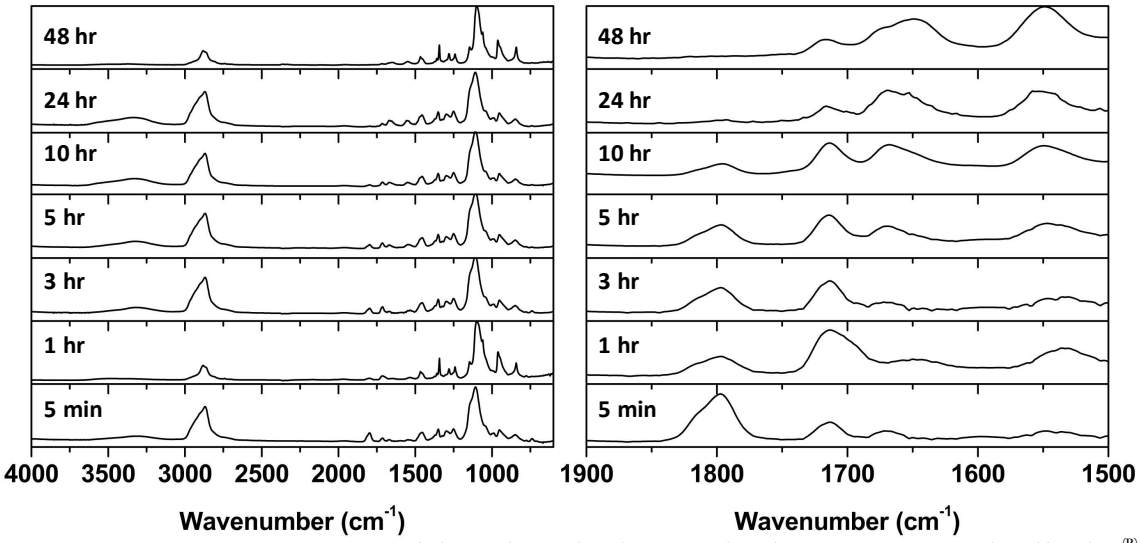

Figure S20. FTIR-ATR spectra of the polymerization reaction between DGC and Jeffamine® ED-2003 at 120°C using TBD as catalyst.

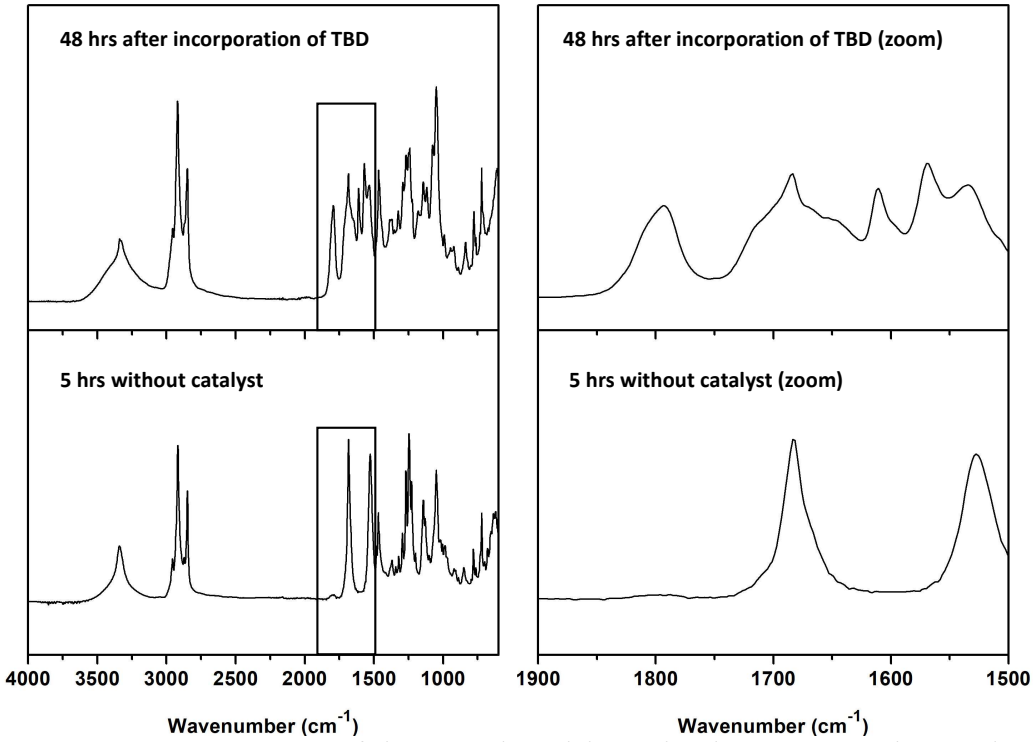

Figure S21. FTIR-ATR spectra of the control model reaction between propylene carbonate and dodecylamine at 120°C after 5 hr without catalyst (until complete conversion of propylene carbonate into urethane) and 48 hr after incorporation of TBD as catalyst.

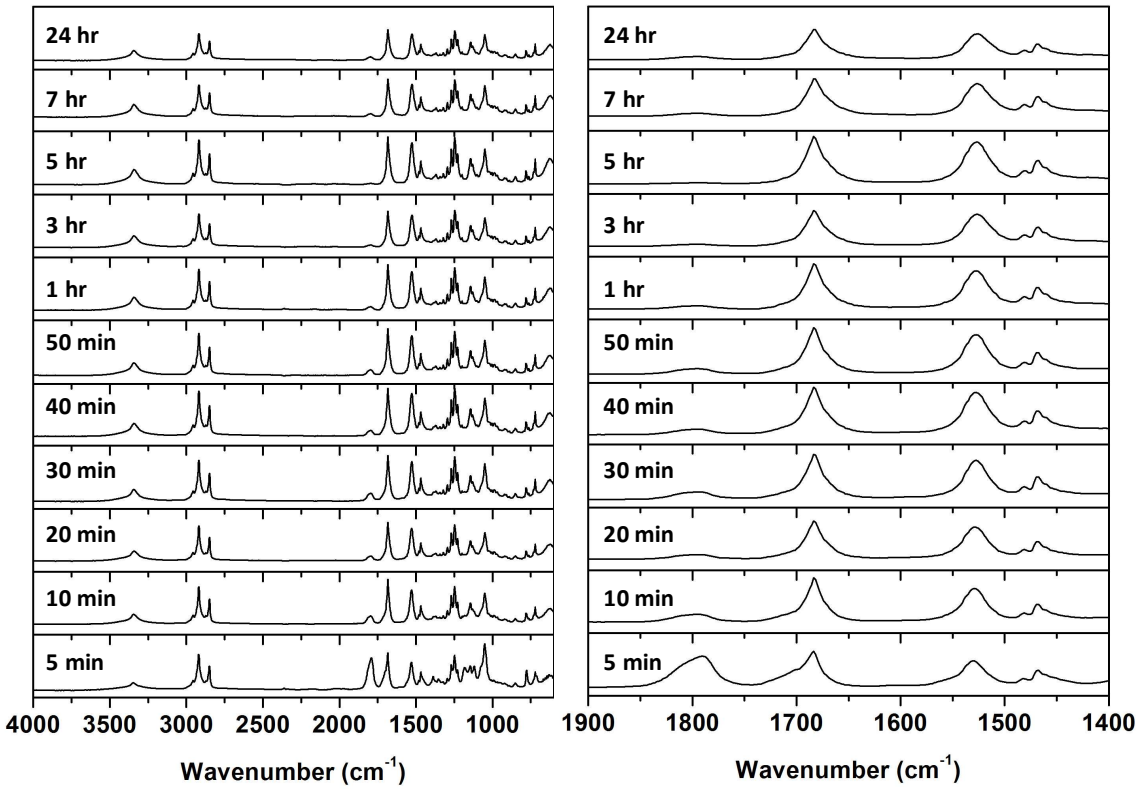

Figure S22. FTIR-ATR spectra of the aminolysis of propylene carbonate with dodecylamine at 120°C using no catalyst.

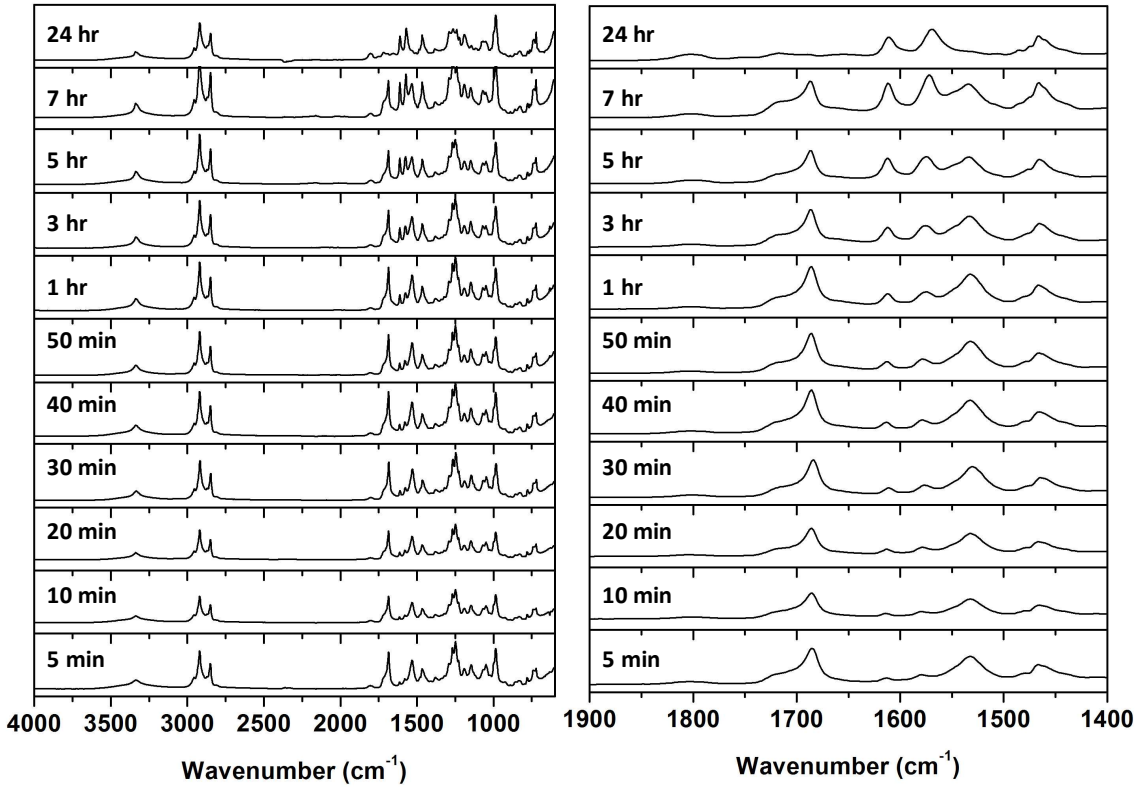

Figure S23. FTIR-ATR spectra of the aminolysis of propylene carbonate with dodecylamine at 120°C using TBD as catalyst.

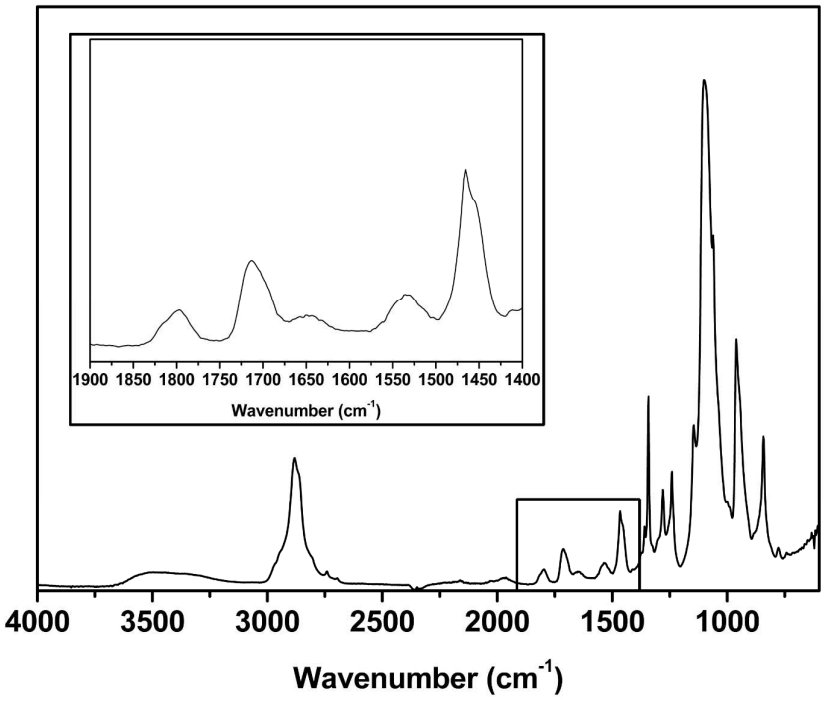

Figure S24. FTIR-ATR spectra of PHUU1

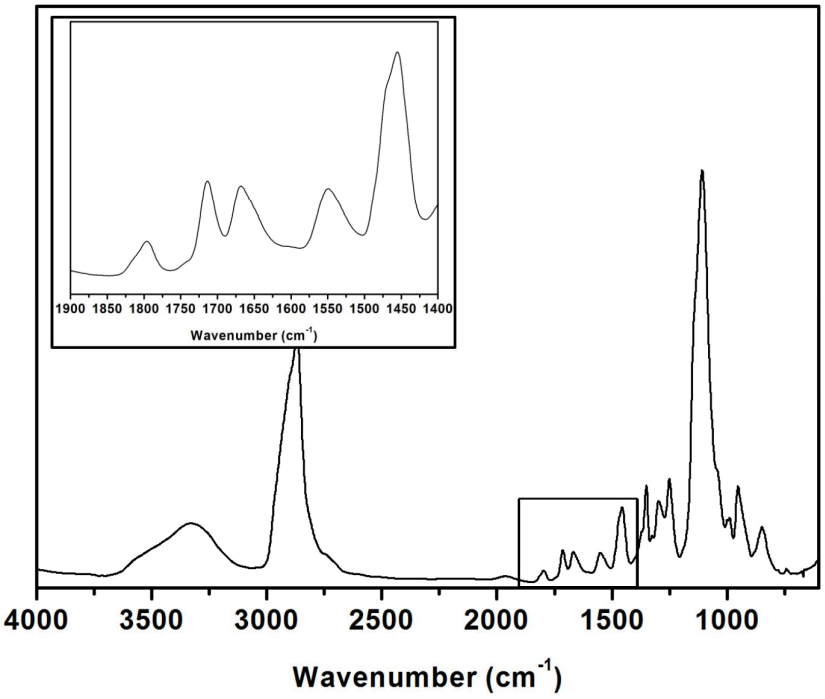

Figure S25. FTIR-ATR spectra of PHUU2

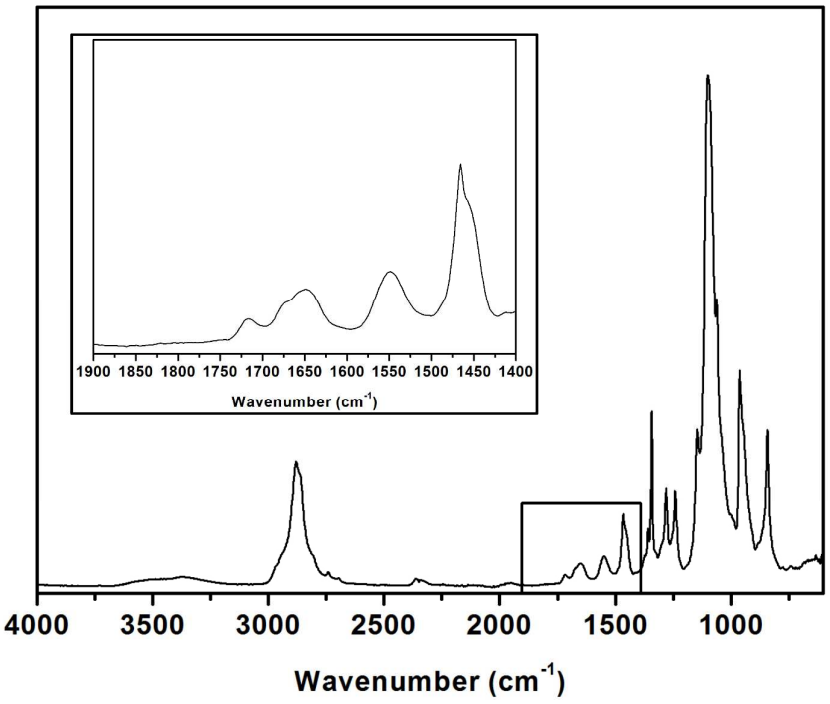

Figure S26. FTIR-ATR spectra of PHUU3

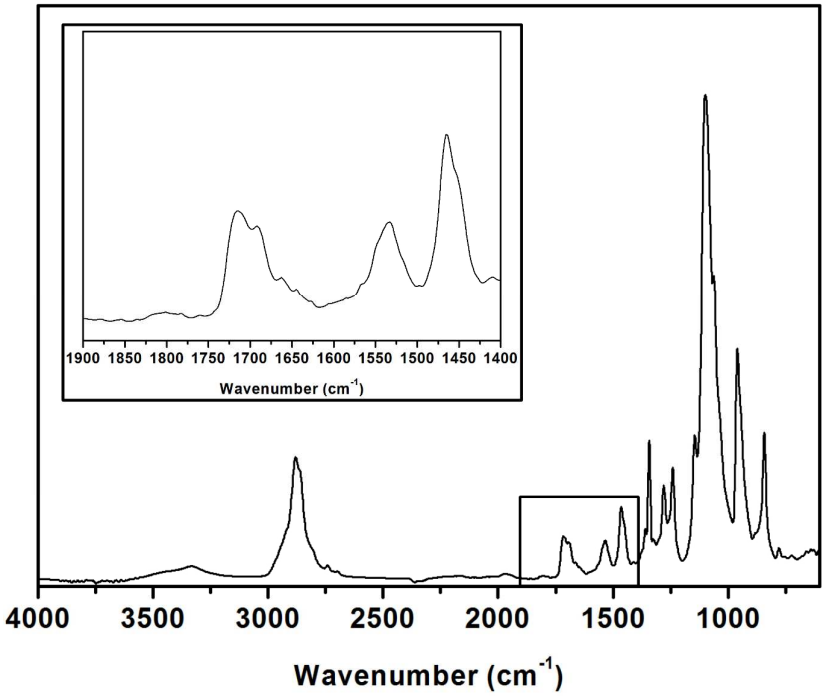

Figure S27. FTIR-ATR spectra of PHUU4

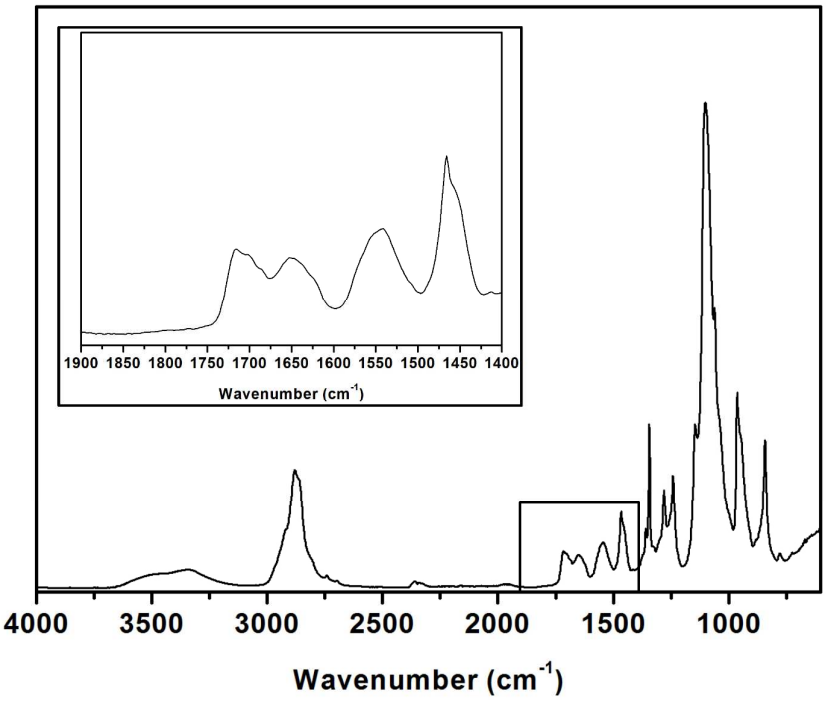

Figure S28. FTIR-ATR spectra of PHUU5

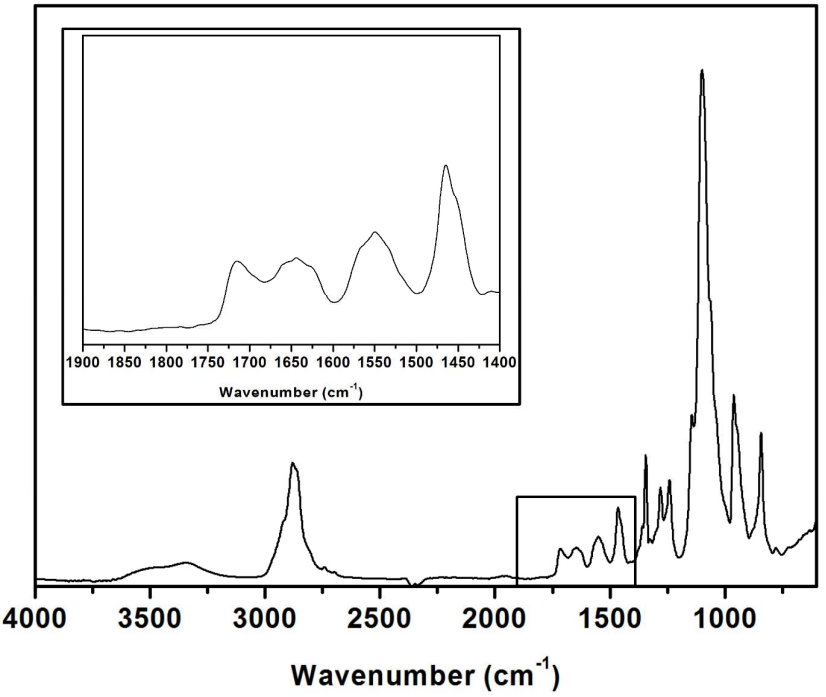

Figure S29. FTIR-ATR spectra of PHUU6

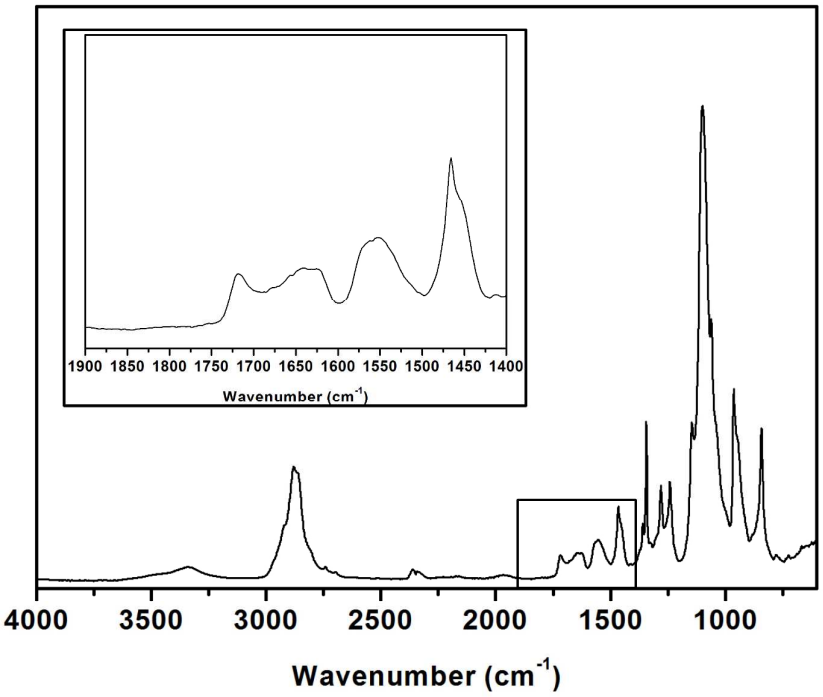

Figure S30. FTIR-ATR spectra of PHUU7

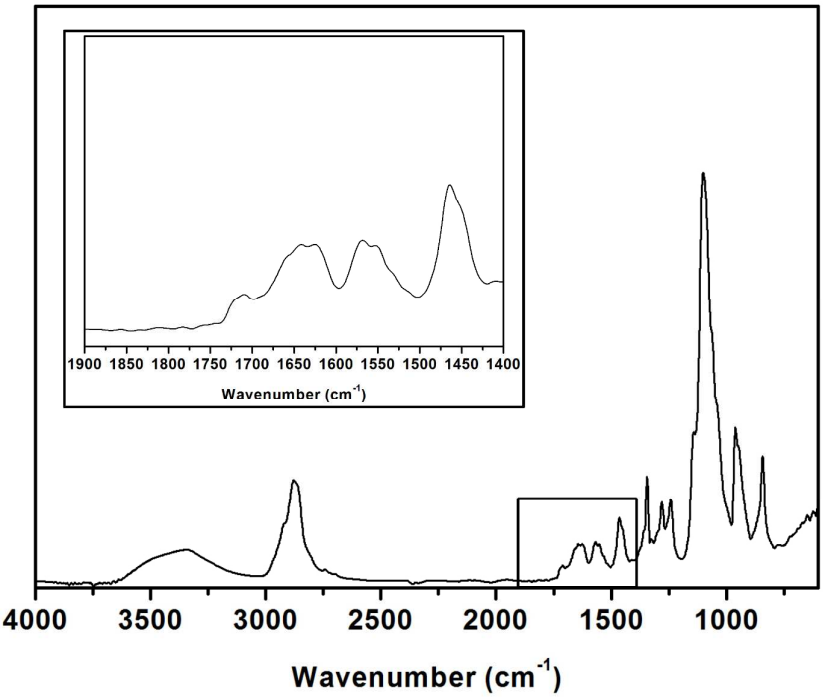

Figure S31. FTIR-ATR spectra of PHUU8

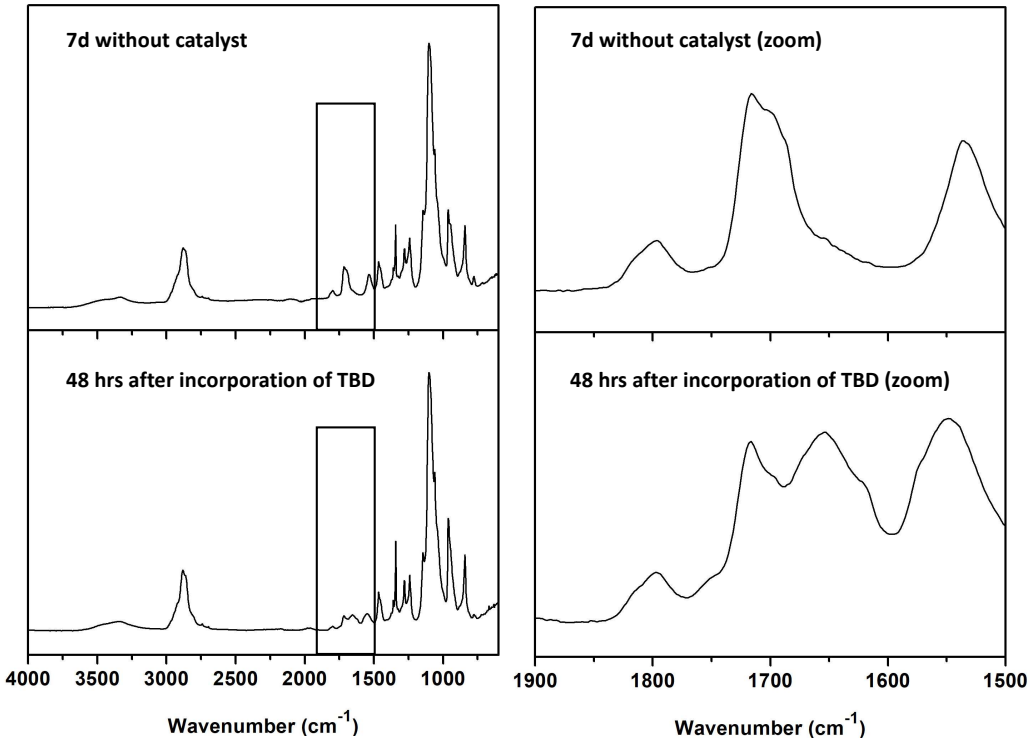

Figure S32. FTIR-ATR spectra of the control polymerization between DGC (1 equiv.), Jeffamine (0.6 equiv.) and 1,12-diaminododecane (0.4 equiv.) at 120°C after 7 days without catalyst (88% urethane conversion) and 48 hr after incorporation of TBD as catalyst (Urea/urethane ratio 69/31).

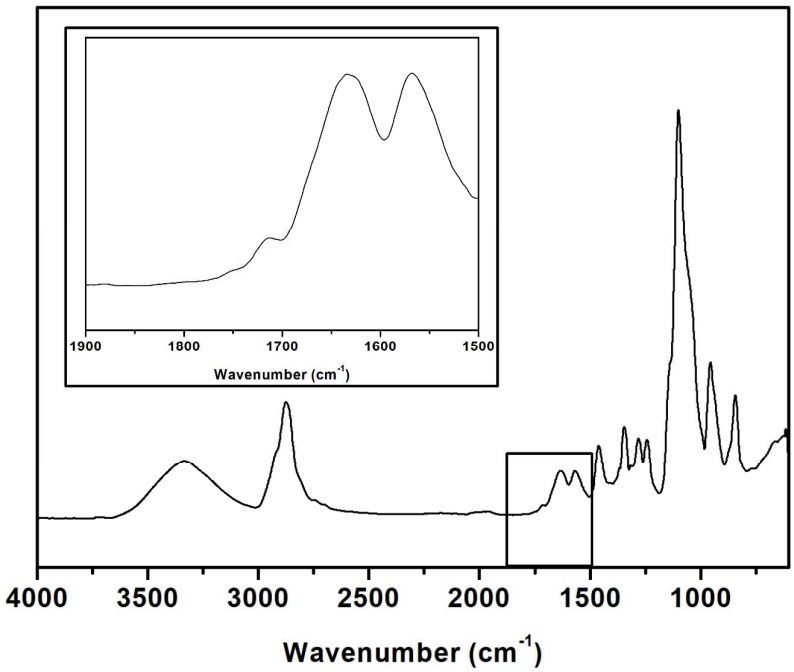

Figure S33. FTIR-ATR spectra of the PHUU obtained from the polymerization of DGC (1 equiv.), Jeffamine (0.6 equiv.) and 1,12-diaminododecane (0.4 equiv.) at 120°C in the presence of 10 mol% of TBD after 7 days for reaching full urea conversion (Urea/urethane ratio 95/5). After 7 days, the reaction mixture became solid preventing to achieve higher urea ratio.

Part 3: LC-TOF-MS and elemental analysis

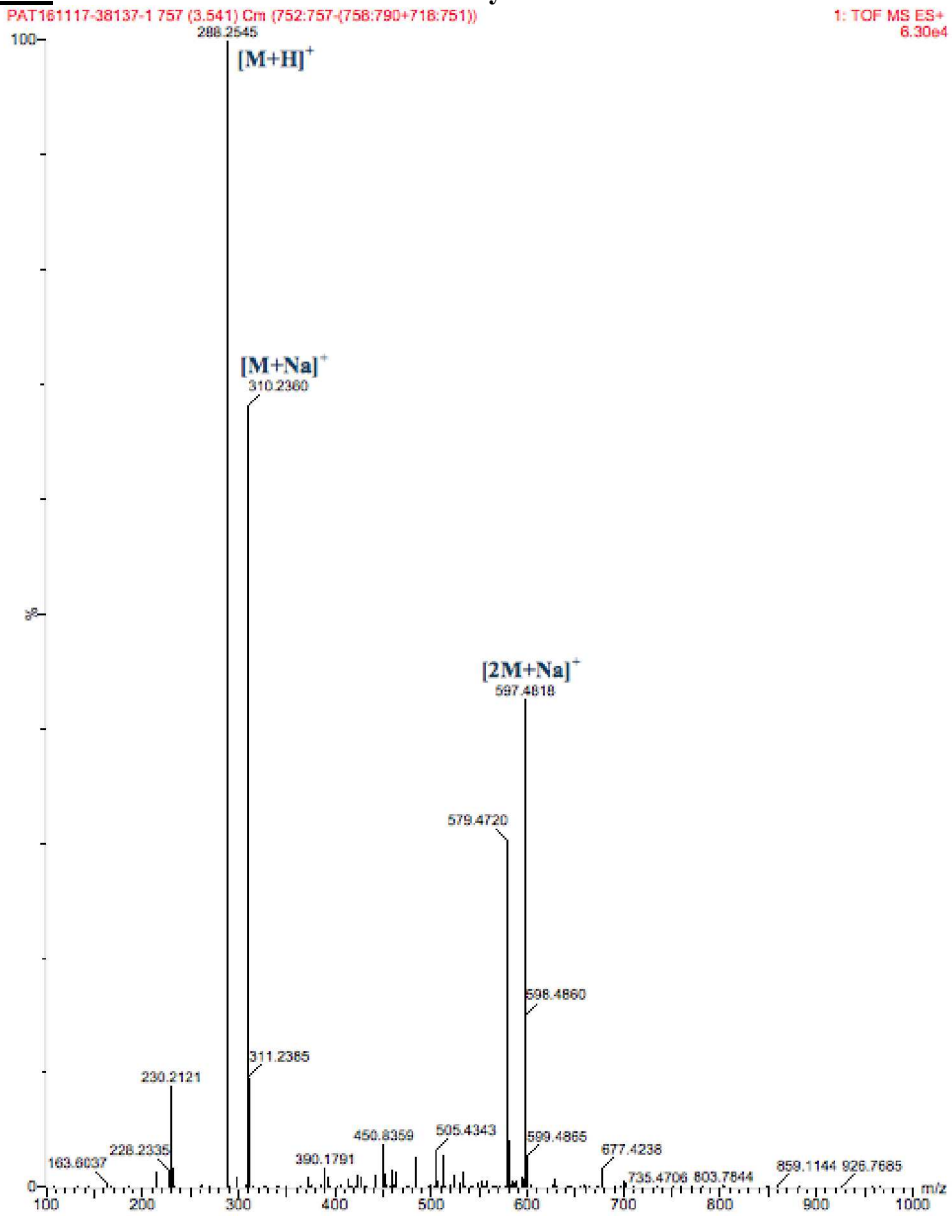

Figure S34. Mass spectra of the molecule from the aminolysis of propylene carbonate with dodecylamine at 120°C using TBD as catalyst eluted after 3.5 min.

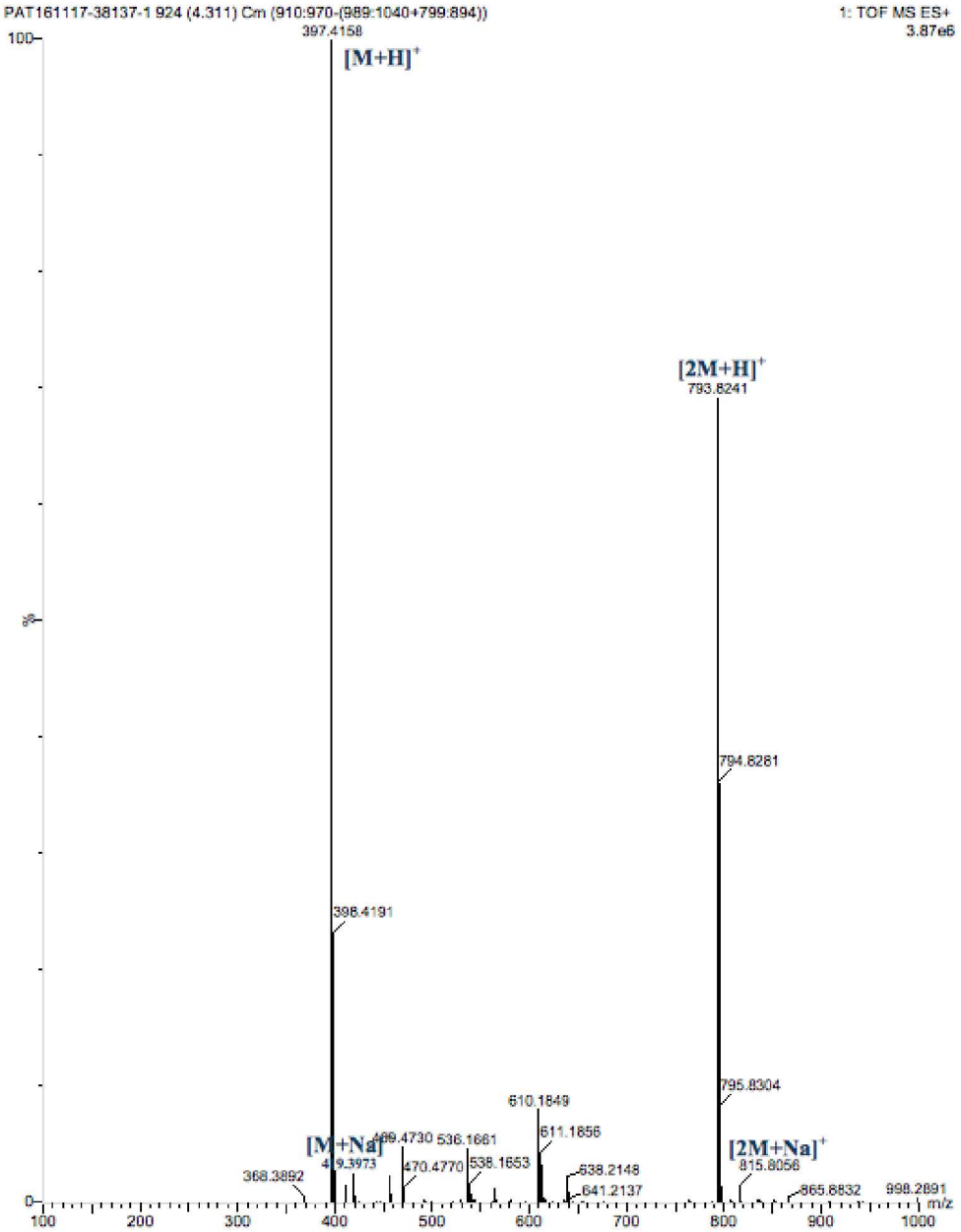

Figure S35. Mass spectra of the molecule from the aminolysis of propylene carbonate with dodecylamine at 120°C using TBD as catalyst eluted after 4.3 min.

Table S1. Elemental analysis results from the aminolysis of propylene carbonate with dodecylamine at 120°C using TBD as catalyst after 24 hours. Experimental values are matching with the chemical formulas of 1,3-didodecylurea.

Elemental composition	C	H	N
Experimental value (%)	75.1	13.4	6.9
Theoretical value (%)	75.7	13.2	7.1

Part 4: Gel permeation chromatography data

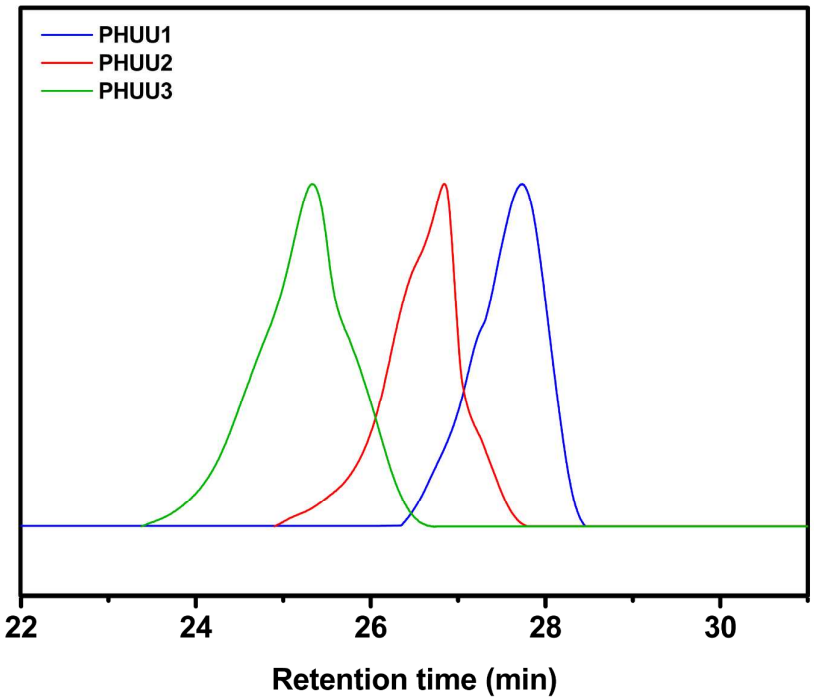

Figure S36. GPC traces of PHUU1, PHUU2 and PHUU3.

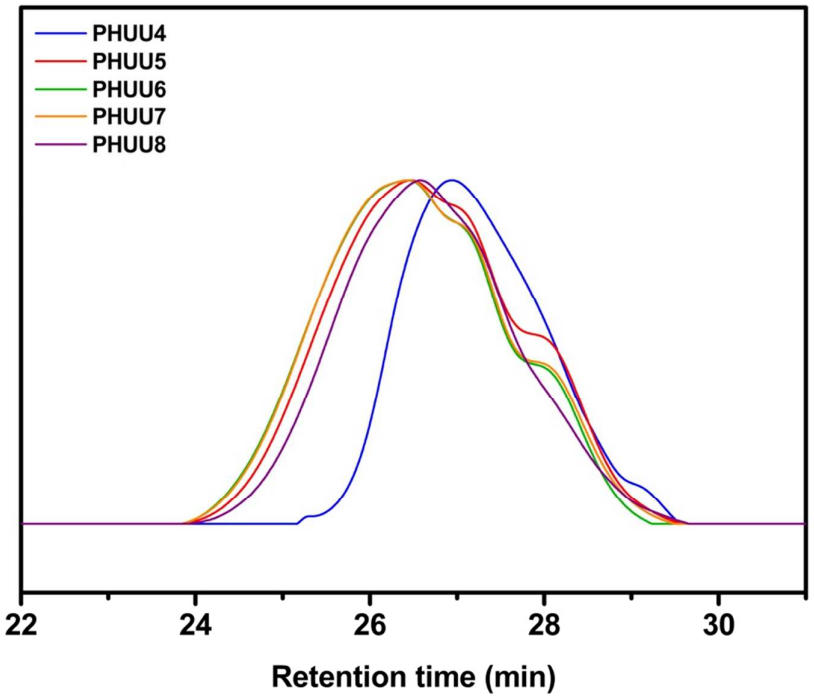

Figure S37. GPC traces of PHUU4, PHUU5, PHUU6, PHUU7 and PHUU8.

Part 5: Differential scanning calorimetry data

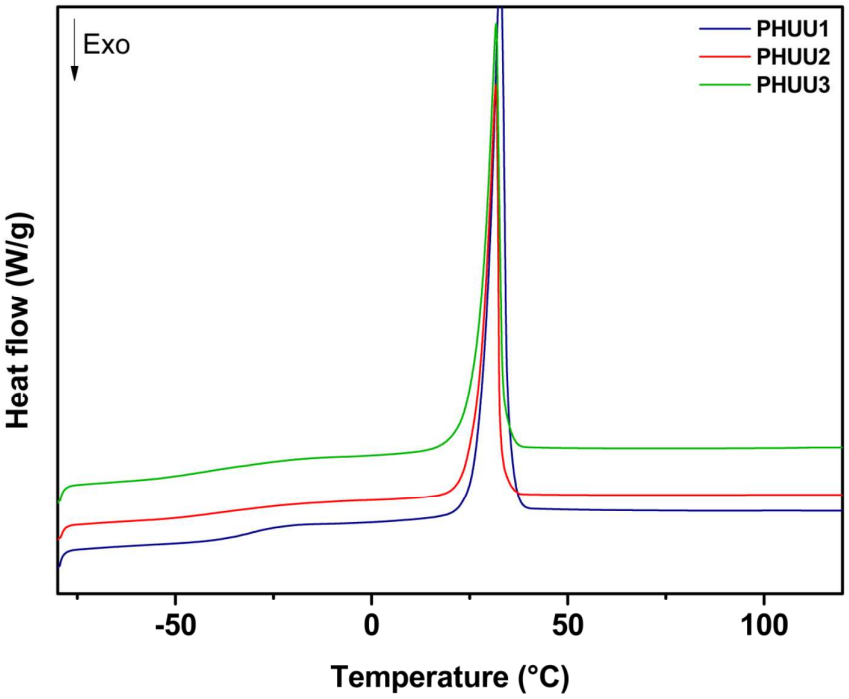

Figure S38. DSC curves of PHUU1, PHUU2 and PHUU3.

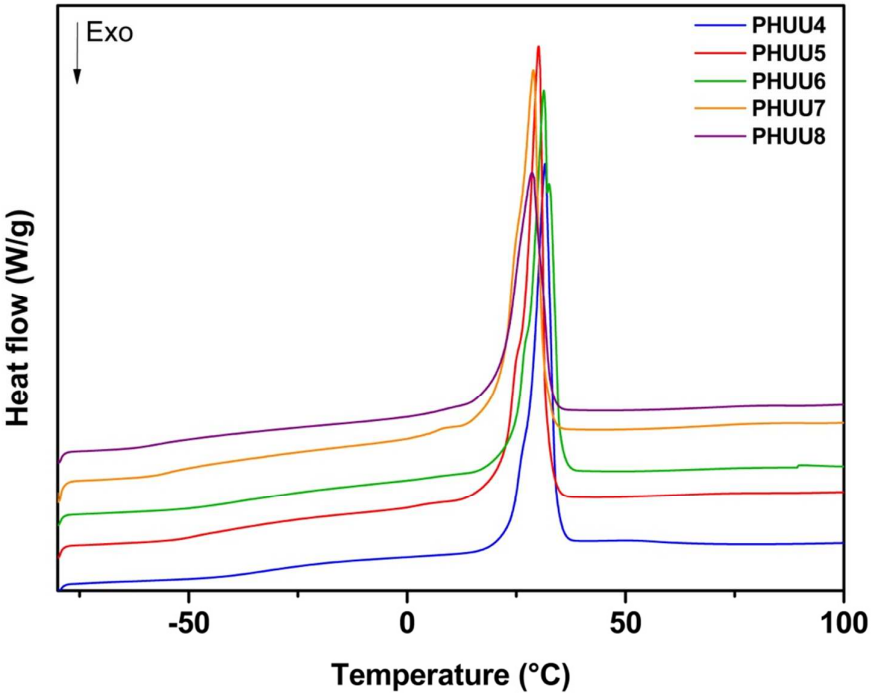

Figure S39. DSC curves of PHUU4, PHUU5, PHUU6, PHUU7 and PHUU8.

Part 6: Kinetic of urea formation at different temperatures

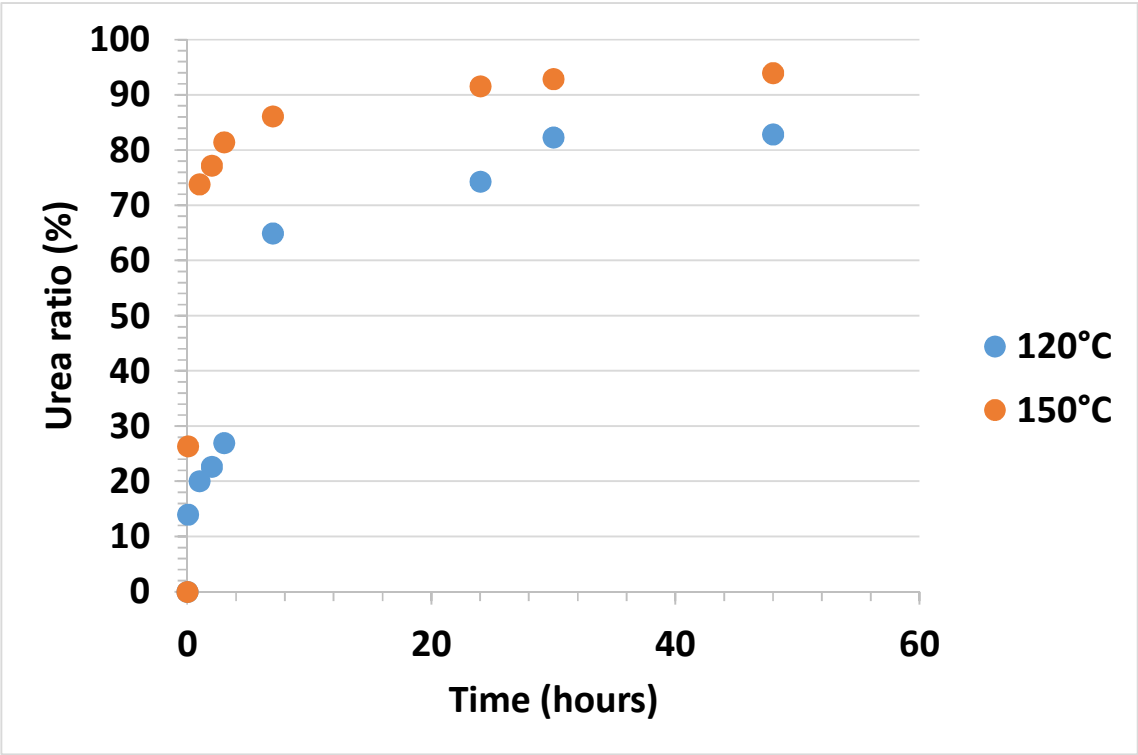

Figure S40. Kinetic of urea formation followed by FTIR over 48 hours at different temperatures from the reaction of DGC with Jeffamine ED-2003 in the presence of 10 mol% of TBD catalyst.